RESEARCH ARTICLE

Global analysis of differential gene expression within the porcine conceptus transcriptome as it transitions through spherical, ovoid, and tubular morphologies during the initiation of elongation

Sophie C. Walsh[1] | Jeremy R. Miles[2] | Brittney N. Keel[2] | Lea A. Rempel[2] | Elane C. Wright-Johnson[2] | Amanda K. Lindholm-Perry[2] | William T. Oliver[2] | Angela K. Pannier[1]

[1]Department of Biological Systems Engineering, University of Nebraska-Lincoln, Lincoln, Nebraska, USA

[2]U.S. Meat Animal Research Center, Clay Center, Nebraska, USA

Correspondence
Jeremy R. Miles, U.S. Meat Animal Research Center, Clay Center, NE 68933, USA.
Email: jeremy.miles@usda.gov

Angela K. Pannier, Department of Biological Systems Engineering, University of Nebraska-Lincoln, Lincoln, NE 68583, USA.
Email: apannier2@unl.edu

Abstract

This study aimed to identify transcriptome differences between distinct or transitional stage spherical, ovoid, and tubular porcine blastocysts throughout the initiation of elongation. We performed a global transcriptome analysis of differential gene expression using RNA-Seq with high temporal resolution between spherical, ovoid, and tubular stage blastocysts at specific sequential stages of development from litters containing conceptus populations of distinct or transitional blastocysts. After RNA-Seq analysis, significant differentially expressed genes (DEGs) and pathways were identified between distinct morphologies or sequential development stages. Overall, 1898 significant DEGs were identified between distinct spherical and ovoid morphologies, with 311 total DEGs between developmental stages throughout this first morphological transition, while 15 were identified between distinct ovoid and tubular, with eight total throughout these second morphological transition developmental stages. The high quantity of DEGs and pathways between conceptus stages throughout the spherical to ovoid transition suggests the importance of gene regulation during this first morphological transition for initiating elongation. Further, extensive DEG coverage of known elongation signaling pathways was illustrated from spherical to ovoid, and regulation of lipid signaling and membrane/ECM remodeling across these early conceptus stages were implicated as essential to this process, providing novel insights into potential mechanisms governing this rapid morphological change.

KEYWORDS
conceptus elongation, porcine, RNA-Seq, transcriptome, uterine environment

1 | INTRODUCTION

During the preimplantation period of porcine conceptus development, the conceptus undergoes a dramatic transformation from a spherical morphology (~1–2 mm), through ovoid (~3–9 mm), and tubular (>10 mm) morphologies, and finally to a long, thin filament (>100 mm) between Days 9 and 12 of gestation (Bazer et al., 1982; Geisert et al., 1982; Miles et al., 2008; Pope & First, 1985). Once initiated, this process of conceptus elongation is very rapid, with the remodeling of the trophoblast and changes in conceptus length occurring at a rate of 35–40 mm per hour on Days 11–12 (Bazer et al., 1988). During elongation, both the conceptus and maternal uterine endometrium undergo extensive changes in gene expression that are essential for the establishment of pregnancy, and for providing a favorable uterine environment for conceptus growth and development (Waclawik et al., 2017). These gene expression changes involve crosstalk between the maternal endometrium and the conceptus, as molecular factors produced by each influence gene expression and morphological changes of the conceptus via the stimulation of signaling cascades (Geisert et al., 2014). Successful conceptus elongation is critical for subsequent embryonic development and survival, as deficiencies in elongation contribute to an estimated 20% of embryonic loss (Pope, 1994) and directly influence within-litter birth weight variability and postnatal piglet survival (Vallet et al., 2009). However, there is currently a lack of understanding of the factors and mechanisms critical to successful elongation in the pig, particularly during the initiation of elongation. Therefore, a more complete understanding of the changes in porcine conceptus gene expression contributing to successful elongation is essential for increasing the overall efficiency of porcine reproduction.

Thus far, previous studies have elucidated a handful of genes undergoing substantial changes in expression between certain porcine conceptus morphologies throughout elongation, including aromatase (CYP19A1) (Blomberg et al. 2005, 2006; Green et al., 1995; Miles et al., 2008; Yelich et al., 1997b), steroid 17-alpha-hydroxylase (CYP17A1) (Yelich et al., 1997b), cytochrome P450 side chain cleavage (CYP11A1) (Blomberg et al., 2005; Miles et al., 2008), steroidogenic acute regulatory protein (STAR) (Blomberg et al. 2005, 2006; Lee et al., 2005; Miles et al., 2008), transforming growth factor-beta 3 (TGFB3) (Lee et al., 2005; Yelich et al., 1997a), and interleukin 1 beta (IL1B) (Lee et al., 2005; Miles et al., 2008; Ross et al., 2003; 2003), as well as multiple mitochondrial and ribosomal proteins (Blomberg et al. 2005, 2006; Ross et al., 2003). While these previous studies demonstrate the importance of conceptus gene regulation throughout the entirety of the elongation process, the goals of the studies were to compare the global gene expression profiles between spherical, tubular, and filamentous (Ross et al., 2003; Ross et al., 2009), ovoid, tubular, and filamentous (Blomberg et al. 2005, 2006), or spherical, filamentous, and early placental implantation (Zang et al., 2021) blastocysts, or to examine changes in expression of select genes between spherical, ovoid, tubular, and filamentous blastocysts (Green et al., 1995; Lee et al., 2005; Miles et al., 2008; Ross et al., 2003; 2003; Yelich et al., 1997a, 1997b). One

study examining the differential expression of select steroidogenic, cellular differentiation, and immune responsiveness genes between spherical, ovoid, and filamentous porcine blastocysts demonstrated significant changes in the expression of multiple genes from spherical to ovoid blastocysts, as well as from spherical and ovoid to filamentous (Miles et al., 2008). The results of this previous study demonstrate substantial changes in gene expression throughout porcine conceptus elongation, notably between the initial spherical and ovoid morphologies at the first morphological transition (Miles et al., 2008). However, to the best of our knowledge, no studies have been performed to characterize changes in global gene expression between the initial spherical, ovoid, and tubular porcine conceptus morphologies of elongation utilizing RNA sequencing (RNA-Seq) technology, which allows for the nontargeted identification of specific genes differentially regulated between early conceptus stages that potentially drive the drastic morphological changes occurring throughout later elongation stages. As such, the specific gene regulation and global expression patterns contributing to the critical period of rapid initiation of porcine conceptus elongation, specifically throughout the initial spherical, ovoid, and tubular morphological stages, or the mechanisms and pathways by which these genes operate, have not yet been fully elucidated.

Therefore, the current study aimed to further elucidate mechanisms of porcine conceptus elongation by examining differences in global gene expression between distinct spherical, ovoid, and tubular porcine conceptus morphologies as the conceptus progress through the initiation of elongation in vivo, as well as by utilizing heterogeneous conceptus morphological stage pregnancies (i.e., litters containing spherical/ovoid or ovoid/tubular blastocysts) to evaluate changes between transitional development stages at a higher temporal resolution amidst these distinct morphologies. Thus, the overall objectives of this study were to characterize porcine conceptus gene expression changes that occur throughout the initiation of elongation between distinct conceptus morphologies, derived from homogeneous morphological stage pregnancies, and between blastocysts at specific sequential stages of development, derived from homogeneous and heterogeneous morphological stage pregnancies. Specifically, we performed a global transcriptome analysis of differential gene expression between distinct spherical (S), ovoid (O), and tubular (T) conceptus morphologies, derived from litters containing homogeneous morphological stage blastocysts, using RNA-Seq to better understand the mechanisms governing the rapid morphological changes that occur during the initiation of porcine conceptus elongation (Figure 1). Additionally, we performed a global transcriptome analysis of differential gene expression with higher temporal resolution between blastocysts at specific sequential stages of development from litters containing homogeneous spherical (S), heterogeneous spherical (S_{T1}) and ovoid (O_{T1}), homogeneous ovoid (O), heterogeneous ovoid (O_{T2}) and tubular (T_{T2}), or homogeneous tubular (T) stage blastocysts using RNA-Seq to establish profiles of select significantly differentially expressed genes (DEGs) identified between distinct porcine conceptus morphologies with increased temporal precision, uncovering potential conceptus mechanisms of gene regulation driving the initiation of elongation (Figure 1).
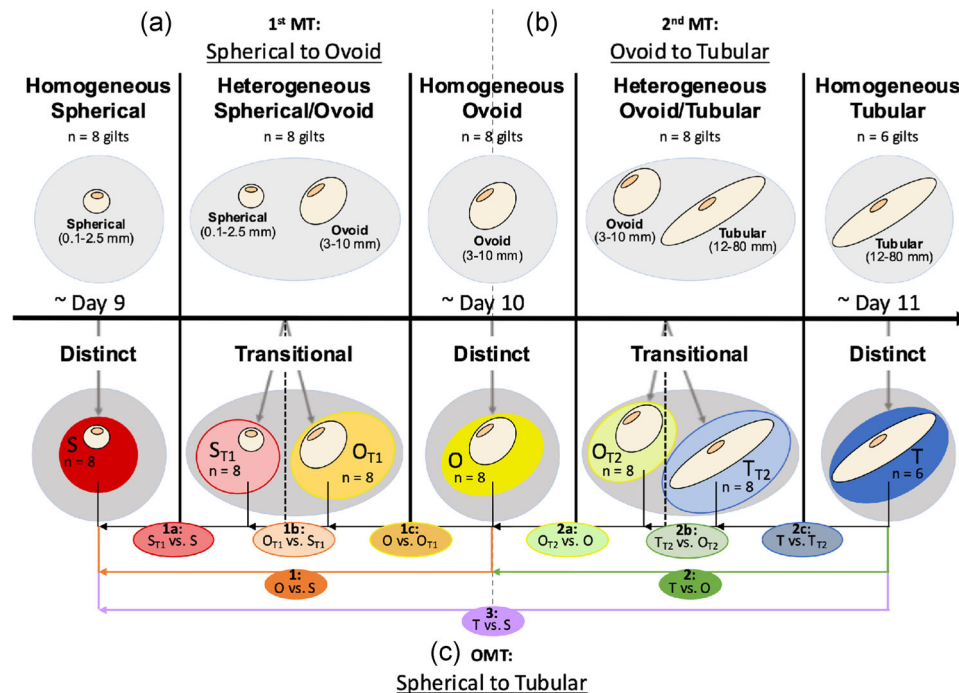
FIGURE 1 Comparisons among distinct and transitional conceptus morphological stages analyzed with RNA-Seq to examine porcine conceptus transcriptome differences throughout the initiation of elongation. Blastocysts were collected from pregnant gilts harvested on Days 9–11 of gestation and classified into spherical, ovoid, and tubular morphological stages according to conceptus morphology and length. Conceptus populations of individual litters were classified according to the uniformity of the most advanced conceptus morphological stage present within the respective litter. Individual blastocysts from these homogeneous and heterogeneous pregnancies were further selected and sorted into conceptus treatment groups based on conceptus morphological stage and conceptus morphological stage uniformities of corresponding litters: distinct spherical blastocysts (S, $n = 8$ blastocysts), from homogeneous spherical stage pregnancies ($n = 8$ gilts); transitional spherical blastocysts (S_{T1}, $n = 8$ blastocysts) or transitional ovoid blastocysts (O_{T1}, $n = 8$ blastocysts) during the first morphological transition, from the same heterogeneous spherical/ovoid stage pregnancies ($n = 8$ gilts); distinct ovoid blastocysts (O, $n = 8$ blastocysts), from homogeneous ovoid stage pregnancies ($n = 8$ gilts); transitional ovoid blastocysts (O_{T2}, $n = 8$ blastocysts) or transitional tubular blastocysts (T_{T2}, $n = 8$ blastocysts) during the second morphological transition, from the same heterogeneous ovoid/tubular stage pregnancies ($n = 8$ gilts); or distinct tubular blastocysts (T, $n = 6$ blastocysts), from homogeneous tubular stage pregnancies ($n = 6$ gilts). The average conceptus morphological stage uniformities for each conceptus treatment group were: S = 100%; S_{T1} = 34%; O_{T1} = 66%; O = 100%; O_{T2} = 43%; T_{T2} = 55%; and T = 90%. To identify differences in gene expression between distinct porcine conceptus morphologies throughout the initiation of elongation, global gene expression of individual blastocysts within each distinct conceptus morphological stage treatment group was analyzed using RNA-Seq, and significant DEGs, pathways, BPs, MFs, and CCs were determined between distinct conceptus morphologies (a) at the first morphological transition (1st MT) from S to O (**1**: O vs. S), (b) at the second morphological transition (2nd MT) from O to T (**2**: T vs. O), and (c) across the overall morphological transition (OMT) from S to T (**3**: T vs. S). To characterize changes in gene expression with fine temporal resolution as the porcine conceptus progresses through specific developmental stages during the initiation of elongation, global gene expression of individual blastocysts within each distinct and transitional conceptus morphological stage treatment group was analyzed using RNA-Seq, and significant DEGs, pathways, BPs, MFs, and CCs were determined between blastocysts at sequential stages of development throughout (a) the 1st MT from spherical to ovoid (**1a**: S_{T1} vs. S, **1b**: O_{T1} vs. S_{T1}, and **1c**: O vs. O_{T1}) and (b) the 2nd MT from ovoid to tubular (**2a**: O_{T2} vs. O, **2b**: T_{T2} vs. O_{T2}, and **2c**: T vs. T_{T2})

2 | RESULTS

Blastocysts from homogeneous and heterogeneous pregnancies were sorted into seven conceptus morphological stage treatment groups based on conceptus morphology and length, as shown in Figure 1. Global gene expression of individual blastocysts within each distinct and transitional conceptus treatment group was analyzed using RNA-Seq, and significant DEGs, pathways, biological processes (BPs), molecular functions (MFs), and cellular components (CCs) were determined between conceptus stages throughout the initiation of elongation (Figure 1). Specifically, gene expression was compared between distinct conceptus morphologies: (1) at the first morphological transition (1st MT) from distinct S to distinct O blastocysts (O vs. S) (Figure 1a); (2) at the second morphological transition (2nd MT) from distinct O to distinct T blastocysts (T vs. O) (Figure 1b); and (3) across the overall morphological transition (OMT) from distinct S to distinct T blastocysts (T vs. S) (Figure 1c), to identify differences in gene expression between distinct conceptus morphologies throughout the initiation of elongation. Additionally, to characterize changes in gene expression with fine temporal resolution as the conceptus progresses through specific developmental stages during the initiation of elongation, gene expression was compared between

blastocysts at sequential stages of development throughout 1) the 1st MT: 1a) distinct S and transitional S_{T1} (S_{T1} vs. S), 1b) transitional S_{T1} and transitional O_{T1} (O_{T1} vs. S_{T1}), and 1c) transitional O_{T1} and distinct O (O vs. O_{T1}) (Figure 1a); and 2) the 2nd MT: 2a) distinct O and transitional O_{T2} (O_{T2} vs. O), 2b) transitional O_{T2} and transitional T_{T2} (T_{T2} vs. O_{T2}), and 2c) transitional T_{T2} and distinct T (T vs. T_{T2}) (Figure 1b).

2.1 | Sequencing statistics

RNA-Seq libraries from 54 individual blastocysts within S, S_{T1}, O_{T1}, O, O_{T2}, T_{T2}, and T treatment groups were sequenced together. Over 5.2 billion 75-bp paired-end reads were generated, with an average of 97.9 million reads per library. After trimming adapter sequences and low-quality bases, the resulting high-quality reads were mapped to the Sscrofa 11.1 genome assembly (Genbank Accession GCA_000003025.6) with an average of 99.1% read mapping rate per library. Sequencing statistics for individual libraries are given in Table S1. Computing read counts for each gene and filtering out genes with low read counts resulted in a set of 25,516 genes for downstream analysis.

2.2 | Abundant and similar changes in gene expression occur between distinct O versus S morphologies at the 1st MT and distinct T versus S morphologies across the OMT during the initiation of elongation

Differential gene expression, pathway, and gene ontology (GO) analysis were performed between S and O blastocysts (Figure 1a) and between S and T blastocysts (Figure 1c) to determine significant DEGs, pathways, BPs, MFs, and CCs between distinct conceptus morphologies at the 1st MT and across the OMT

during the initiation of elongation. A total of 1898 genes were significantly differentially expressed between O versus S after false discovery rate (FDR) adjustment ($p \leq 0.05$) and fold change (FC) filtering ($|\log_2 FC| \geq 1$; i.e., FC ≥ 2) (Tables 1 and S2). Of these significant DEGs, 1384 genes were upregulated and 514 were downregulated (Tables 1 and S2) from S to O conceptus morphology (Figure 2a). Between T versus S, 2291 total genes were significantly differentially expressed (Tables 1 and S2), with 1608 DEGs upregulated and 683 downregulated (Tables 1 and S2) from S to T conceptus morphology (Figure 2b). Overall, there was substantial overlap in significant DEGs between the first O versus S and overall T versus S morphological transitions, including in fold change magnitude, direction (up- or downregulation), and putative function of similar DEGs (Tables 1–3), altogether demonstrating the abundance and intensity of altered gene expression at the 1st MT from S to O during the initiation of porcine conceptus elongation. Specifically, many of the most highly differentially expressed genes between O versus S and T versus S function in cytokine signaling pathways, steroidogenesis, and lipid metabolism (Tables 2 and S2), while many of the most highly downregulated DEGs are involved in ECM remodeling and cellular adhesion (Tables 3 and S2).

Pathway analysis identified a total of 29 pathways that were significantly enriched between O versus S conceptus morphologies after FDR adjustment ($p \leq 0.05$) (Tables 1 and 4), and a total of 19 significantly enriched pathways between T versus S (Tables 1 and 5). Substantial overlap in these enriched pathways was observed between the O versus S and T versus S comparisons, with 14 identical pathways and several similarities in pathway functions between 1st MT and OMT distinct morphologies, including pathways related to cytokine and growth factor signaling (e.g., cytokine–cytokine receptor interaction, MAPK signaling pathway, NF-kappa B signaling pathway, PI3K-Akt signaling pathway, HIF-1 signaling pathway), steroidogenesis (e.g., ovarian steroidogenesis, steroid biosynthesis, cholesterol metabolism, regulation of lipolysis in adipocytes),

TABLE 1 Numbers of significant DEGs, pathways, and GO terms between distinct conceptus morphologies (O vs. S, T vs. O, and T vs. S) throughout the initiation of elongation

ANALYSIS		O versus S	T versus O	T versus S	Both O versus S/T versus S
DEGs	Total	1898	15	2291	1480
Upregulated		**1384**	**2**	**1608**	**1095**
Downregulated		(514)	(13)	(683)	(385)
Pathways		29	0	19	14
Biological Processes		996	2	796	636
Molecular Functions		82	6	54	46
Cellular Components		108	0	81	68

Note: DEGs with $p \leq 0.05$ and $|\log2FC| \geq 1$ (i.e., FC ≥ 2) and pathways and GO terms with $p \leq 0.05$ were considered statistically significant; DEGs in bold = upregulated; DEGs within parentheses = downregulated.

Abbreviations: O, distinct ovoid; S, distinct spherical; T, distinct tubular.
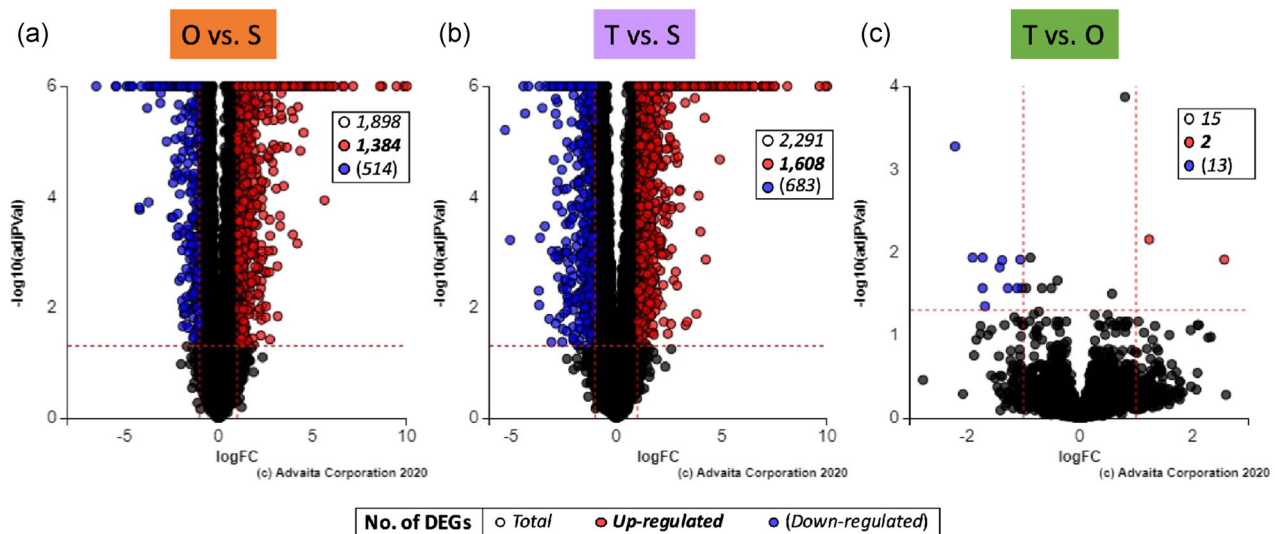
FIGURE 2 Volcano plots of total gene expression changes from (a) distinct S to distinct O (O vs. S), (b) distinct S to distinct T (T vs. S), and (c) distinct O to distinct T (T vs. O) conceptus morphologies throughout the initiation of elongation. $\log_2$FC (x-axis) against p-value (y-axis) of significant DEGs ($p \leq 0.05$ and $|\log_2$FC$| \geq 1$) upregulated (red) and downregulated (blue). All other DEGs with $p > 0.05$ and/or $|\log_2$FC$| < 1$ are indicated in black. Numbers of significant DEGs between conceptus stages are detailed according to the plot legend within boxes overlayed on corresponding volcano plots

phospholipid membrane remodeling (e.g., glycerolipid metabolism, ether lipid metabolism, sphingolipid metabolism, glycerophospholipid metabolism), and ECM remodeling and cellular adhesion (e.g., ECM-receptor interaction, cell adhesion molecules (CAMs), regulation of actin cytoskeleton, focal adhesion) (Tables 4 and 5). GO analysis identified a total of 996 BPs, 82 MFs, and 108 CCs that were significantly enriched between O versus S conceptus morphologies after FDR adjustment ($p \leq .05$), and a total of 796 BPs, 54 MFs, and 81 CCs significantly enriched between T versus S (Tables 1 and Table S3). The most significantly enriched BPs between O versus S and T versus S were mainly terms related to signaling, adhesion, and development (Tables 6 and Table S3), while many of the most significant MFs were terms involving signaling and transport (Tables 7 and S3).

2.3 | Limited changes in gene expression occur between distinct T versus O morphologies at the 2nd MT

Differential gene expression, pathway, and GO analysis were performed between O and T blastocysts (Figure 1b) to determine significant DEGs, pathways, BPs, MFs, and CCs between distinct conceptus morphologies at the 2nd MT during the initiation of elongation. Only 15 genes were found to be significantly differentially expressed ($p \leq 0.05$ and $|\log_2$FC$| \geq 1$) between T versus O conceptus morphologies (Tables 1 and 8); two of these DEGs were upregulated and 13 were downregulated (Tables 1 and 8) from O to T blastocysts (Figure 2c). Additionally, GO analysis identified only two BPs and six MFs (Tables 1 and 9) that were

significantly enriched ($p \leq 0.05$) between T versus O conceptus morphologies, while no pathways or CCs were significantly enriched between T versus O (Table 1). Overall, the DEGs between T versus O function as regulators of a broad range of biological processes in a variety of tissues (Table 8), indicating that the 2nd MT from O to T mainly involves changes in a small number of genes regulating embryonic developmental processes and general metabolism.

2.4 | Moderate changes in gene expression between blastocysts at sequential stages of development throughout the 1st MT (S_{T1} versus S, O_{T1} versus S_{T1}, and O versus O_{T1}) highlight specific DEGs identified between distinct O versus S and T versus S morphologies

Differential gene expression, pathway, and GO analysis were performed from distinct S to distinct O conceptus morphologies between S and S_{T1} blastocysts, between S_{T1} and O_{T1} blastocysts, and between O_{T1} and O blastocysts (Figure 1a) to determine significant DEGs, pathways, BPs, MFs, and CCs between blastocysts at specific sequential stages of development throughout the 1st MT from spherical to ovoid during the initiation of elongation. A total of 101 genes were significantly differentially expressed between S_{T1} versus S after FDR adjustment ($p \leq 0.05$) and FC filtering ($|\log_2$FC$| \geq 1$; i.e., FC ≥ 2) (Tables 10 and S2); among these DEGs, 85 genes were upregulated (Tables 10, 11, and S2) and 16 were downregulated (Tables 10, 12, and S2) from S to S_{T1} blastocysts (Figure 3a). Between O_{T1} versus S_{T1} blastocysts, only three genes were significantly differentially expressed

TABLE 2 Ten most highly upregulated significant DEGs ($p \leq 0.05$ and $|\log_2FC| \geq 1$) between O versus S and T versus S conceptus morphologies throughout the initiation of elongation

Contrast		DEG Symbol	Entrez ID	$\log_2FC$	p-value	Associated Significantly Enriched Pathways ($p \leq .05$)	DEG upregulated in both O versus S/T versus S?
O versus S	1.	*CYP19A1*	13075	13.04	4.69E−103	Metabolic pathways; Ovarian steroidogenesis	No
	2.	*LOC110259014*		10.96	7.86E−10	N/A	No
	3.	*CYP17A1*	13074	9.84	7.92E−145	Metabolic pathways; Ovarian steroidogenesis	Yes
	4.	*IL1B*	16176	9.45	1.40E−13	MAPK signaling pathway; NF-kappa B signaling pathway; Cytokine−cytokine receptor interaction; Hematopoietic cell lineage	Yes
	5.	*LOC110258125*		9.12	6.56E−15	N/A	Yes
	6.	*LOC110258579*		8.74	1.62E−16	N/A	Yes
	7.	*LOC110255300*		8.72	3.95E−54	N/A	Yes
	8.	*IFNG*	15978	8.70	6.83E−31	Cytokine−cytokine receptor interaction; Pathways in cancer; HIF-1 signaling pathway	Yes
	9.	*IL1B2*		8.61	1.03E−63	N/A	Yes
	10.	*SLC27A6*	225579	8.58	3.72E−22	X	Yes
T versus S	1.	*CYP17A1*	13074	10.55	9.10E−197	Metabolic pathways	Yes
	2.	*IL1B*	16176	9.90	1.46E−09	Cytokine−cytokine receptor interaction; MAPK signaling pathway; NF-kappa B signaling pathway; Th17 cell differentiation	Yes
	3.	*LOC110258125*		9.67	1.54E−11	N/A	Yes
	4.	*SLC27A6*	225579	9.63	5.18E−35	X	Yes
	5.	*LOC110258579*		9.23	6.49E−13	N/A	Yes
	6.	*LOC110255300*		9.20	1.60E−38	N/A	Yes
	7.	*IL1B2*		9.12	1.94E−44	N/A	Yes
	8.	*LOC110258095*		8.67	1.74E−39	N/A	Yes
	9.	*LOC110258582*		8.19	1.64E−33	N/A	Yes
	10.	*ANKRD33B*	67434	8.12	3.47E−88	X	Yes

Abbreviations: O, distinct ovoid; S, distinct spherical; T, distinct tubular.

(Tables 10–12), with two DEGs upregulated (Tables 10 and 11), and one downregulated (Tables 10 and 12) from S_{T1} to O_{T1} blastocysts (Figure 3b). Lastly, a total of 221 genes were significantly differentially expressed between O versus O_{T1} blastocysts (Tables 10 and S2), 118 of which were upregulated (Tables 10, 11, and S2) and 103 downregulated (Tables 10, 12, and S2) from O_{T1} to O blastocysts (Figure 3c). These results demonstrate that most of the significant DEGs between blastocysts at sequential stages of development throughout the 1st MT from S to O occurred between developmental stages of the same conceptus morphological stage (i.e., between S_{T1} vs. S or O vs. O_{T1}), as opposed to at the morphological transformation from S_{T1} to O_{T1} (i.e., O_{T1} vs. S_{T1}), which had limited deviation in gene expression between differing morphological stages within a similar uterine environment (i.e., heterogeneous spherical/ovoid stage litters). Additionally, 290 of the DEGs detected between S_{T1} versus S, O_{T1} versus S_{T1}, and O versus O_{T1} blastocysts

(constituting 93% of the significant DEGs between developmental stages throughout the 1st MT) were also significant DEGs identified between distinct O versus S morphologies (each with identical directions of fold change across the developmental stage and distinct morphology comparisons) (Tables 10–12), identifying specific genes with rapid and substantial expression changes that may function as essential regulators driving the initiation of porcine conceptus elongation.

Pathway analysis identified significant enrichment after FDR adjustment ($p \leq 0.05$) of 23 pathways between S_{T1} versus S blastocysts, seven pathways between O_{T1} versus S_{T1}, and one pathway between O versus O_{T1} (Tables 10 and 13). These enriched pathways between S_{T1} versus S, O_{T1} versus S_{T1}, and O versus O_{T1} overlapped considerably with the enriched pathways identified between O versus S, with eight identical pathways and several similarities in pathway functions between 1st MT developmental stages and distinct O versus S morphologies, many of

TABLE 3 Ten most highly downregulated significant DEGs ($p \leq .05$ and $|log_2FC| \geq 1$) between O versus S and T versus S conceptus morphologies throughout the initiation of elongation

Contrast		DEG Symbol	Entrez ID	log_2FC	p-value	Associated Significantly Enriched Pathways ($p \leq 0.05$)	DEG downregulated in both O versus S/T versus S?
O versus S	1.	(*GULO*)	268756	−6.49	1.95E−38	Metabolic pathways; Ascorbate and aldarate metabolism	Yes
	2.	(*ST6GALNAC1*)	20445	−5.46	7.99E−44	Metabolic pathways	Yes
	3.	(*IGSF5*)	72058	−5.43	1.56E−08	X	Yes
	4.	(*SERPINE1*)	18787	−4.87	3.55E−28	HIF-1 signaling pathway	Yes
	5.	(*FUT1*)	14343	−4.74	4.92E−36	Metabolic pathways	Yes
	6.	(*BTN1A1*)	12231	−4.73	3.81E−24	X	Yes
	7.	(*CEMIP*)	80982	−4.64	4.34E−40	X	Yes
	8.	(*CASS4*)	320664	−4.58	4.23E−13	X	Yes
	9.	(*COLCA2*)	100502940	−4.21	1.56E−04	X	No
	10.	(*SCIN*)	20259	−4.19	1.73E−04	Regulation of actin cytoskeleton	Yes
T versus S	1.	(*LIPH*)	239759	−5.27	6.19E−06	X	No
	2.	(*IGSF5*)	72058	−5.03	6.06E−04	X	Yes
	3.	(*SCIN*)	20259	−4.39	6.71E−10	X	Yes
	4.	(*GULO*)	268756	−4.32	3.11E−06	Metabolic pathways	Yes
	5.	(*ST6GALNAC1*)	20445	−4.16	1.10E−07	Metabolic pathways	Yes
	6.	(*GALNTL5*)	67909	−3.67	5.01E−03	Metabolic pathways	Yes
	7.	(*P2RX1*)	18436	−3.65	9.12E−03	X	Yes
	8.	(*CASS4*)	320664	−3.64	1.01E−10	X	Yes
	9.	(*FREM1*)	329872	−3.61	5.55E−04	ECM-receptor interaction	No
	10.	(*GABBR2*)	242425	−3.50	2.48E−06	X	Yes

Abbreviations: O, distinct ovoid; S, distinct spherical; T, distinct tubular.

which are related to cytokine and growth factor signaling and steroidogenesis (Table 13). Lastly, GO analysis identified significant enrichment after FDR adjustment ($p \leq 0.05$) of 92 BPs and 10 CCs between S_{T1} versus S blastocysts, 20 BPs and 20 MFs between O_{T1} versus S_{T1}, and 24 BPs, 10 MFs, and 6 CCs between O versus O_{T1} (Tables 10 and S3). No MFs were significantly enriched between S_{T1} versus S, and no CCs were significantly enriched between O_{T1} versus S_{T1} (Table 10).

2.5 | Limited changes in gene expression occur between blastocysts at sequential stages of development throughout the 2nd MT (O_{T2} vs. O, T_{T2} vs. O_{T2}, and T vs. T_{T2})

Differential gene expression, pathway, and GO analysis were performed from distinct O to distinct T conceptus morphologies between O and O_{T2} blastocysts, between O_{T2} and T_{T2} blastocysts, and between T_{T2} and T blastocysts (Figure 1b) to determine significant DEGs, pathways, BPs, MFs, and CCs between blastocysts at specific

sequential stages of development throughout the 2nd MT from ovoid to tubular during the initiation of elongation. Only three genes were significantly differentially expressed ($p \leq 0.05$ and $|log_2FC| \geq 1$) between O_{T2} versus O blastocysts (Tables 10 and 14), all of which were downregulated (Tables 10 and 14) from O to O_{T2} (Figure 3d). Between T_{T2} versus O_{T2} blastocysts, only four genes were significantly differentially expressed (Tables 10 and 14), two of which were upregulated and two downregulated (Tables 10 and 14) from O_{T2} to T_{T2} blastocysts (Figure 3e). Lastly, only two genes were significantly differentially expressed between T versus T_{T2} blastocysts (Tables 10 and 14), both of which were upregulated (Tables 10 and 14) from T_{T2} to T (Figure 3f).

Pathway analysis of these DEGs identified significant enrichment ($p \leq 0.05$) of five pathways between O_{T2} versus O blastocysts and one pathway between T versus T_{T2} (Tables 10 and S3). No pathways were significantly enriched between T_{T2} versus O_{T2} (Table 10). GO analysis identified significant enrichment ($p \leq 0.05$) of 127 BPs and 12 MFs between O_{T2} versus O blastocysts, 37 BPs between T_{T2} versus O_{T2}, and 1 BP and 5 MFs between T versus T_{T2} (Tables 10 and S3). No MFs were significantly enriched between T_{T2} versus O_{T2}, and no CCs

TABLE 4 Significantly enriched pathways ($p \leq .05$) between O versus S conceptus morphologies during the initiation of elongation

	Pathway	DE/All Genes	p-value	Pathway DEGs (Highest|log₂FC|)[a]	Pathway sig. in T versus S?
1.	MAPK signaling pathway	41/212	1.20E−02	*IL1B, CACNA2D3, TGFB3, IGF2, DUSP9, DUSP5, ERBB4, MAP3K8, EFNA5, RASGRF1*, etc.	Yes
2.	Glycerolipid metabolism	16/44	1.20E−02	*LPIN1, MBOAT2, PLPP1, MOGAT1, DGKH,* (*ALDH9A1*), *MGLL,* (*AKR1A1*), *ALDH1B1, PLPP2*, etc.	Yes
3.	Metabolic pathways	172/1022	1.55E−02	*CYP19A1, CYP17A1, HSD11B2,* (*GULO*), *ALOX12,* (*ST6GALNAC1*), *ATP12A, ACER2,* (*FUT1*), *LPIN1*, etc.	Yes
4.	Regulation of lipolysis in adipocytes	12/30	1.55E−02	*IRS1, IRS2, LIPE,* (*PTGS2*), *GNAI1, MGLL, NPR1, INSR, PDE3B, NPY1R*, etc.	No
5.	Cytokine–cytokine receptor interaction	16/82	1.66E−02	*IL1B, IFNG, CXCL12, TGFB3, BMPR1B, GDF6,* (*TNFSF4*), *TNFRSF11A, TNFRSF13C,* (*TNFSF9*), etc.	Yes
6.	Cholesterol metabolism	14/35	1.66E−02	*STAR, APOB,* (*SOAT1*), *MYLIP, SORT1,* (*NPC1*), *SOAT2, LPL, LRP1,* (*STARD3*), etc.	No
7.	NF-kappa B signaling pathway	14/67	1.66E−02	*IL1B, CXCL12,* (*BTK*), (*PTGS2*), *TICAM1, TNFRSF11A, DDX58, TNFRSF13C,* (*EDARADD*), (*GADD45B*), etc.	Yes
8.	Axon guidance	34/135	1.70E−02	*CXCL12, ABLIM1, BMPR1B, WNT4, EFNA5, SRGAP3, PAK3, GNAI1, UNC5A,* (*NTNG1*), etc.	No
9.	Dilated cardiomyopathy (DCM)	17/53	1.70E−02	*CACNA2D3, TGFB3, SLC8A1, IGF1, CACNB2,* (*CACNA2D1*), *ITGA3,* (*ITGA9*), *ITGA6, MYBPC3*, etc.	Yes
10.	Sphingolipid metabolism	14/42	1.87E−02	*ACER2, CERS6, SPTLC3, PLPP1,* (*GAL3ST1*), *SGMS1, SPHK1, CERS3, PLPP2, UGT8*, etc.	Yes
11.	Hypertrophic cardiomyopathy (HCM)	16/52	1.95E−02	*CACNA2D3, TGFB3, SLC8A1, IGF1, CACNB2,* (*CACNA2D1*), *ITGA3,* (*ITGA9*), *ITGA6, MYBPC3*, etc.	Yes
12.	Amoebiasis	13/50	2.47E−02	*IL1B, IFNG, TGFB3,* (*ARG1*), *LAMA3, NOS2, GNA15, FN1, LAMB3,* (*PRKCB*), etc.	Yes
13.	Regulation of actin cytoskeleton	32/157	2.81E−02	*CHRM3, CXCL12, MYLK,* (*SCIN*), *DIAPH2, FGF10, TMS84X, PAK3, F2, CHRM4*, etc.	No
14.	Neuroactive ligand–receptor interaction	23/80	2.81E−02	*CHRM3,* (*P2RX1*), *PTGER4,* (*GABRD*), (*GABBR2*), *LPAR3, F2, CHRM4,* (*S1PR5*), *P2RX7*, etc.	Yes
15.	Ether lipid metabolism	11/31	2.81E−02	*PLPP1,* (*GAL3ST1*), *GDPD1, LPCAT1, PLPP2,* (*LPCAT2*), *PLA2G12B, UGT8, PLD2, PAFAH2*, etc.	Yes
16.	Pathways in cancer	68/366	2.92E−02	*IFNG, CXCL12, TGFB3, PTGER4, IGF2, WNT4, GNG11, PPARG, GNGT1, DLL1*, etc.	Yes
17.	Hematopoietic cell lineage	9/23	2.92E−02	*IL1B,* (*TFRC*), (*KITLG*), *CD44, ITGA3, ITGA6,* (*CD59*), *ITGA2,* (*CD9*)	No
18.	PI3K-Akt signaling pathway	42/214	4.20E−02	*MAGI2, IGF2, GNG11, GNGT1, LAMA3, ERBB4, EFNA5, FGF10, COL9A1, IRS1*, etc.	No
19.	HIF-1 signaling pathway	16/79	4.20E−02	*IFNG,* (*SERPINE1*), *NOS2, IGF1, PFKFB3, HKDC1, CDKN1A, HK3,* (*TFRC*), *INSR*, etc.	No
20.	Morphine addiction	15/48	4.20E−02	*GNG11,* (*GABRD*), (*GABBR2*), *GNGT1,* (*PDE11A*), *PDE10A, GNAI1,* (*PDE3A*), *GABBR1, PDE3B*, etc.	No
21.	Cell adhesion molecules (CAMs)	15/54	4.20E−02	*CLDN3,* (*ICOSLG*), *IGSF11, NRXN1, CADM1, CD86,* (*NTNG1*), *CLDN1,* (*CDH3*), (*SDC4*), etc.	Yes
22.	ECM-receptor interaction	14/44	4.20E−02	*LAMA3, COL9A1, NPNT, FN1, LAMB3,* (*SDC4*), *CD44, ITGA3,* (*ITGA9*), *ITGA6*, etc.	Yes

TABLE 4 (Continued)

	Pathway	DE/All Genes	p-value	Pathway DEGs (Highest|log$_2$FC|)[a]	Pathway sig. in T versus S?
23.	Ovarian steroidogenesis	10/25	4.20E-02	**CYP19A1, CYP17A1, STAR, HSD17B1**, (PTGS2), **IGF1, INSR, IGF1R, ADCY6, LDLR**	No
24.	Gastric acid secretion	10/39	4.20E-02	**CHRM3, MYLK, KCNJ15, KCNJ2, GNAI1**, (ITPR1), (PRKCB), **ITPR3, ADCY6, CAMK2G**	No
25.	Steroid biosynthesis	7/17	4.20E-02	(SOAT1), **LSS, SOAT2, CYP51, SQLE, TM7SF2, DHCR24**	No
26.	Intestinal immune network for IgA production	6/14	4.20E-02	**CXCL12** , (ICOSLG), **CD86, TNFRSF13C, AICDA, TGFB1**	No
27.	Type I diabetes mellitus	5/7	4.20E-02	**IL1B, IFNG, CD86, ICA1**, (CPE)	No
28.	Ascorbate and aldarate metabolism	5/9	4.20E-02	(GULO), (ALDH9A1), **ALDH1B1**, (RGN), (MIOX)	No
29.	Pancreatic secretion	9/41	4.37E-02	**CLCA2, CHRM3, RAB27B, SLC26A3**, (ITPR1), **PLA2G12B**, (PRKCB), **ITPR3, ADCY6**	No

Abbreviations: O, distinct ovoid; S, distinct spherical; T, distinct tubular.

[a]Pathway DEGs are listed in order of highest to lowest |log$_2$FC|; DEGs in bold = upregulated; DEGs within parentheses = downregulated; pathways with > 10 significant DEGs list only the 10 DEGs with highest |log$_2$FC|followed by etc.

were significantly enriched between O$_{T2}$ versus O, T$_{T2}$ versus O$_{T2}$, or T versus T$_{T2}$ (Table 10).

3 | DISCUSSION

This study characterized differences in global gene expression of the porcine conceptus between distinct S, O, and T morphologies, as well as between specific sequential stages of conceptus development throughout the first (S, S$_{T1}$, O$_{T1}$, and O) and second (O, O$_{T2}$, T$_{T2}$, and T) morphological transitions at high temporal resolution amidst distinct conceptus morphologies, utilizing RNA-Seq and bioinformatic analysis of blastocysts derived from homogeneous and heterogeneous morphological stage pregnancies. Overall, the results of this study: (1) indicate that extensive changes in gene expression and related pathways occur throughout the 1st MT from S to O morphology during the initiation of porcine conceptus elongation, while remaining limited throughout the 2nd MT from O to T, potentially implicating this 1st MT as most critical in guiding the initiation of elongation; and (2) identify specific DEGs with substantial and rapid changes in expression between sequential development stages throughout the 1st MT that may function as essential regulators driving the initiation of elongation. Together, these results: (i) illustrate extensive DEG coverage of molecular signaling pathways (i.e., cytokine and growth factor signaling and steroidogenesis pathways) known to play important roles in porcine conceptus elongation; (ii) implicate conceptus regulation of phospholipid membrane remodeling and lipid signaling pathways as potential mechanisms essential to elongation in the pig; and (iii) suggest that the adhesion cascade involving ECM remodeling, which has been well characterized around the time of porcine conceptus implantation, may begin during the initiation of elongation.

3.1 | Cytokine and growth factor signaling and steroidogenesis

During the preimplantation period of porcine conceptus development, signaling molecules such as cytokines, growth factors, and estrogens produced by the conceptus and maternal endometrium are essential mechanisms of the extensive crosstalk at the conceptus-maternal interface via the stimulation of signaling cascades (Geisert et al., 2014). This crosstalk between the maternal endometrium and conceptus results in the induction of factors essential to survival and elongation of the conceptus through changes in gene expression and molecular factor secretion of both the uterine endometrium and developing conceptus (Waclawik et al., 2017). In the current study, many of the most highly differentially expressed genes and significantly enriched pathways between distinct morphology (O vs. S) and sequential developmental (S$_{T1}$ vs. S, O$_{T1}$ vs. S$_{T1}$, O$_{T1}$ to O) conceptus stages throughout the 1st MT, as well as between distinct T versus S morphologies across the OMT, are directly involved in cytokine and growth factor signaling (Figure 4; Table S4). These

TABLE 5 Significantly enriched pathways ($p \leq 0.05$) between T versus S conceptus morphologies during the initiation of elongation

	Pathway	DE/All Genes	p-value	Pathway DEGs (Highest|log$_2$FC|)[a]	Pathway sig. in O versus S?
1.	Ether lipid metabolism	17/31	3.79E−04	**PLPP1, GDPD1**, (GAL3ST1), (PLB1), **PLPP2, PLA2G12B, LPCAT1, ENPP2, UGT8**, (LPCAT2), etc.	Yes
2.	Protein digestion and absorption	18/39	2.25E−03	**SLC8A1, SLC9A3, MEP1B, SLC6A19, SLC16A10**, (COL27A1), **COL11A1, SLC15A1**, (DPP4), **COL4A2**, etc.	No
3.	Cytokine–cytokine receptor interaction	23/80	3.09E−03	**IL1B, TGFB3, IFNG, CXCL12, BMPR1B, TNFRSF11A, GDF11, IL17B, GDF6, LIF**, etc.	Yes
4.	Neuroactive ligand-receptor interaction	27/73	3.81E−03	**PTGER4**, (P2RX1), **LPAR3**, (GABBR2), (GABRD), **CHRM4, GABBR1, ADORA2A, P2RX7, SSTR1**, etc.	Yes
5.	Pathways in cancer	88/365	4.51E−03	**TGFB3, IFNG, CXCL12, PPARG, MGST1, PTGER4, IGF2, LPAR3, WNT4, NOTCH3**, etc.	Yes
6.	MAPK signaling pathway	47/210	4.51E−03	**IL1B, TGFB3, CACNA2D3, IGF2, DUSP9, DUSP5, FGF10, EFNA5, RASGRF1, IGF1**, etc.	Yes
7.	Amoebiasis	17/48	4.51E−03	**IL1B, TGFB3, IFNG, LAMA3, PLCB1**, (ARG1), **LAMB3, FN1, GNA15, TGFB1**, etc.	Yes
8.	Sphingolipid metabolism	17/42	7.32E−03	**ACER2, CERS6, PLPP1, SPTLC3, SGMS1, SPHK1**, (GAL3ST1), **CERS3, PLPP2, ARSA**, etc.	Yes
9.	ECM-receptor interaction	19/45	1.30E−02	(FREM1), **LAMA3, LAMB3, FN1, ITGA6, NPNT, CD44, CD47**, (SDC4), **ITGA3**, etc.	Yes
10.	NF-kappa B signaling pathway	16/66	2.25E−02	**IL1B, CXCL12**, (PTGS2), **TICAM1, TNFRSF11A**, (BTK), **DDX58, TNFRSF13C**, (EDARADD), **TNFAIP3**, etc.	Yes
11.	Glycerophospholipid metabolism	23/74	3.28E−02	**LPGAT1, LPIN1, MBOAT2, PLPP1, DGKH, GPAT3**, (PLB1), **PLPP2, PLA2G12B, CHKA**, etc.	No
12.	Dilated cardiomyopathy (DCM)	18/52	3.28E−02	**TGFB3, CACNA2D3, SLC8A1, IGF1, ITGA6, TPM4, TGFB1, MYL3, CACNB2, ITGA3**, etc.	Yes
13.	Cell adhesion molecules (CAMs)	18/53	3.28E−02	**CLDN3, CADM1**, (ICOSLG), **CLDN1**, (NTNG1), **ITGA6**, (CLDN8), **CD86, ALCAM**, (SELPLG), etc.	Yes
14.	Glycerolipid metabolism	16/44	3.28E−02	**LPIN1, MBOAT2, PLPP1, DGKH, MOGAT1, MGLL, GPAT3**, (AKR1A1), **PLPP2, AGPAT3**, etc.	Yes
15.	Metabolic pathways	202/1015	3.44E−02	**CYP17A1, HSD11B2, ALOX12, ACER2, ATP12A, ACSS1, LPIN1**, (GULO), **MGST1**, (ST6GALNAC1), etc.	Yes
16.	Focal adhesion	38/131	4.05E−02	**MYLK, LAMA3, PAK3, MYL9, LAMB3, RASGRF1, BAD, IGF1, FN1, TLN1**, etc.	No
17.	Hypertrophic cardiomyopathy (HCM)	17/51	4.31E−02	**TGFB3, CACNA2D3, SLC8A1, IGF1, ITGA6, TPM4, TGFB1, MYL3, CACNB2, ITGA3**, etc.	Yes
18.	Th17 cell differentiation	15/61	4.31E−02	**IL1B, IFNG, CD247, STAT5A, NFATC1, TGFB1, STAT5B, MAPK13, RORA**, (LAT), etc.	No
19.	Inflammatory bowel disease (IBD)	8/21	4.31E−02	**IL1B, TGFB3, IFNG, NFATC1, TGFB1, RORA, JUN, STAT1**	No

Abbreviations: O, distinct ovoid; S, distinct spherical; T, distinct tubular.

[a]Pathway DEGs are listed in order of highest to lowest |log$_2$FC|; DEGs within parentheses = downregulated; pathways with >10 significant DEGs list only the 10 DEGs with highest |log$_2$FC|followed by etc.

TABLE 6 Ten most significantly enriched biological processes ($p \leq 0.05$) between O versus S and T versus S conceptus morphologies throughout the initiation of elongation

Contrast		GO ID	Biological Process (BP)	DE/All Genes	p-value	BP DEGs (Highest|log2FC|)[a]	BP sig. in both O versus S and T versus S? O versus S/T versus S?
O versus S	1.	GO:0032501	Multicellular organismal process	701/4025	5.45E-19	*CYP19A1, IL1B, IFNG, HSD11B2, ADGRL3, FRY, RBP4, ALOX12, CHRM3, CXCL12*, etc.	Yes
	2.	GO:0051239	Regulation of multicellular organismal process	390/1958	5.91E-17	*CYP19A1, IL1B, IFNG, ADGRL3, RBP4, ALOX12, CHRM3, CXCL12, GRHL3, SCUBE2*, etc.	Yes
	3.	GO:0009653	Anatomical structure morphogenesis	360/1801	1.30E-15	*IL1B, IFNG, CRISPLD2, FRY, RBP4, ALOX12, CXCL12, GRHL3, MYLK, MYO18B*, etc.	Yes
	4.	GO:0048731	System development	520/2887	6.14E-15	*CYP19A1, IL1B, IFNG, ADGRL3, FRY, RBP4, ALOX12, CXCL12, GRHL3, MYLK*, etc.	Yes
	5.	GO:0023052	Signaling	564/3196	6.54E-15	*CYP19A1, IL1B, IFNG, ADGRL3, RBP4, CHRM3, CXCL12, GRHL3, NEURL1B, SCUBE2*, etc.	Yes
	6.	GO:0048856	Anatomical structure development	609/3530	1.82E-14	*CYP19A1, IL1B, IFNG, ADGRL3, CRISPLD2, FRY, RBP4, ALOX12, CXCL12, GRHL3*, etc.	Yes
	7.	GO:0007154	Cell communication	566/3241	4.55E-14	*CYP19A1, IL1B, IFNG, ADGRL3, RBP4, CHRM3, CXCL12, GRHL3, NEURL1B, SCUBE2*, etc.	Yes
	8.	GO:0007155	Cell adhesion	181/757	7.27E-14	*IL1B, IFNG, CLCA2, ADGRL3, ALOX12, CXCL12, (IGSF5), ACER2, (SERPINE1), (BTN1A1)*, etc.	Yes
	9.	GO:0007275	Multicellular organism development	564/3239	7.82E-14	*CYP19A1, IL1B, IFNG, ADGRL3, FRY, RBP4, ALOX12, CXCL12, GRHL3, MYLK*, etc.	Yes
	10.	GO:0030154	Cell differentiation	458/2508	7.82E-14	*IL1B, IFNG, ADGRL3, FRY, CXCL12, MYO18B, SCUBE2, (SERPINE1), IRX3, TGM1*, etc.	Yes
T versus S	1.	GO:0007155	Cell adhesion	216/739	3.12E-15	*IL1B, IFNG, CXCL12, ADGRL3, ALOX12, ACER2, CLDN3, SLC7A11, (IGSF5), PDPN*, etc.	Yes
	2.	GO:0022610	Biological adhesion	216/743	3.17E-15	*IL1B, IFNG, CXCL12, ADGRL3, ALOX12, ACER2, CLDN3, SLC7A11, (IGSF5), PDPN*, etc.	Yes
	3.	GO:0051239	Regulation of multicellular organismal process	454/1931	4.87E-15	*IL1B, TGFB3, IFNG, CXCL12, ADGRL3, GRHL3, ALOX12, FOXA1, RBP4, IRX3*, etc.	Yes
	4.	GO:0032501	Multicellular organismal process	820/3964	5.36E-15	*IL1B, TGFB3, IFNG, CXCL12, ADGRL3, HSD11B2, GRHL3, ALOX12, FOXA1, RBP4*, etc.	Yes
	5.	GO:0007154	Cell communication	683/3190	8.18E-15	*IL1B, TGFB3, IFNG, CXCL12, ADGRL3, GRHL3, NEURL1B, FOXA1, ACER2, RBP4*, etc.	Yes
	6.	GO:0023052	Signaling	672/3144	2.60E-14	*IL1B, TGFB3, IFNG, CXCL12, ADGRL3, GRHL3, NEURL1B, FOXA1, ACER2, RBP4*, etc.	Yes

(Continues)

TABLE 6 (Continued)

Contrast		GO ID	Biological Process (BP)	p-value	DE/All Genes	BP DEGs (Highest|log₂FC|)[a]	BP sig. in both O versus S/T versus S?
	7.	GO:0030155	Regulation of cell adhesion	1.03E−13	142/439	*IL1B, IFNG, CXCL12, ALOX12, ACER2, PDPN, TDGF1, MAGI2, PTGER4, IGF2*, etc.	Yes
	8.	GO:0007165	Signal transduction	1.83E−12	619/2902	*IL1B, TGFB3, IFNG, CXCL12, ADGRL3, GRHL3, NEURL1B, FOXA1, ACER2, TAGAP*, etc.	Yes
	9.	GO:0032879	Regulation of localization	3.68E−12	416/1807	*IL1B, TGFB3, IFNG, CXCL12, ALOX12, RBP4, IGFBP3, KCNJ15, CACNA2D3, PPARG*, etc.	Yes
	10.	GO:0009653	Anatomical structure morphogenesis	4.09E−12	408/1767	*IL1B, TGFB3, IFNG, CXCL12, GRHL3, ALOX12, FOXA1, RBP4, IRX3, PPARG*, etc.	Yes

Abbreviations: O, distinct ovoid; S, distinct spherical; T, distinct tubular.

[a]BP DEGs are listed in order of highest to lowest |log₂FC|; DEGs in bold = upregulated; DEGs within parentheses = downregulated; only the 10 DEGs with highest |log₂FC| are listed for each BP, followed by etc.

results included the differential expression of *IL1B* genes, interferon-gamma (*IFNG*), C-X-C motif chemokine ligand 12 (*CXCL12*), genes involved in fibroblast growth factor (FGF) and insulin-like growth factor (IGF) signaling, *TGFB1*, *TGFB3*, and retinol-binding protein 4 (*RBP4*) between 1st MT conceptus stages and T versus S morphologies within NF-kappa B, MAPK, PI3K-Akt, HIF-1, and TGF-beta signaling pathways. Altered expression and enrichment of many of these genes and associated pathways have been previously identified at the time of conceptus elongation and implantation in the pig (Geisert et al., 2014; Waclawik et al., 2017), in agreement with the current findings. However, the current results further demonstrate extensive DEG coverage across these enriched pathways that has not yet been reported. Thus, the high-fold expression changes of the above DEGs and enrichment of the above pathways between conceptus stages within the 1st MT and OMT in the current study emphasize the extensive maternal-conceptus crosstalk during this period of development, while implicating specific cytokines and growth factors as essential components of key signaling pathways presumed to facilitate porcine conceptus elongation via modulation of the uterine inflammatory and immune response, stimulation of trophectoderm cell migration, proliferation, and differentiation, induction of tissue remodeling, and regulation of cellular adhesion and ECM reorganization (Geisert et al., 2001; Geisert et al., 2014; Han et al., 2018; Jeong et al., 2014; Ka et al., 2001; Massuto et al., 2010; Yelich et al., 1997a).

Additionally, a number of genes within enriched pathways related to steroidogenesis and cholesterol metabolism were significantly differentially expressed between conceptus stages throughout the 1st MT and across the OMT in the current study (Figure 5a; Table S4), including differential expression of several steroidogenic transcripts and genes involved in uptake, transport, and mobilization of cholesterol (Chang et al., 2017; Du et al., 2011; Hong et al., 2010; McLeod & Yao, 2016; Strauss & FitzGerald, 2019) between 1st MT conceptus stages and T versus S morphologies. Increased estrogen synthesis and secretion by the porcine conceptus during elongation, accompanied by upregulation of several steroidogenic transcripts, has been well characterized (Blomberg et al., 2005). However, the DEG coverage across the multiple steroidogenic pathways illustrated in the current study is more extensive than identified by previous studies. Therefore, the differential expression of steroidogenic and cholesterol-related genes within the current study provides further support for the crucial role of steroid hormone production by the porcine conceptus in the establishment of pregnancy and successful initiation of conceptus elongation (Bazer & Johnson, 2014).

3.2 | Phospholipid membrane remodeling and lipid signaling

In the current study, numerous DEGs within multiple enriched pathways related to phospholipid metabolism indicate potential remodeling of the trophectoderm as the conceptus transitions from S

TABLE 7 Ten most significantly enriched molecular functions ($p \leq 0.05$) between O versus S and T versus S conceptus morphologies throughout the initiation of elongation

Contrast	No.	GO ID	Molecular Function (MF)	DE/All Genes	p-value	MF DEGs (Highest|log$_2$FC|)[a]	MF sig. in both O versus S/T versus S?
O versus S	1.	GO:0038023	Signaling receptor activity	99/356	2.81E−10	*ADGRL3, CHRM3, TDGF1,* (P2RX1), (ESRRG), *PTGER4, BMPR1B,* (CASR), (GABRD), *PPARG,* etc.	Yes
	2.	GO:0004888	Transmembrane signaling receptor activity	79/269	2.06E−09	*ADGRL3, CHRM3,* (P2RX1), *PTGER4, BMPR1B,* (CASR), (GABRD), *NPSR1,* (GABBR2), *ERBB4,* etc.	Yes
	3.	GO:0005215	Transporter activity	141/614	7.96E−09	*SLC27A6, CLCA2, RBP4, ATP12A, CACNA2D3, KCNJ15, STAR, SLC15A2, ABCA12, SLC8A1,* etc.	Yes
	4.	GO:0060089	Molecular transducer activity	102/399	7.96E−09	*ADGRL3, CHRM3, TDGF1,* (P2RX1), (ESRRG), *PTGER4, BMPR1B,* (CASR), (GABRD), *PPARG,* etc.	Yes
	5.	GO:0022857	Transmembrane transporter activity	122/544	4.28E−07	*CLCA2, RBP4, ATP12A, CACNA2D3, KCNJ15, SLC15A2, ABCA12, SLC8A1,* (P2RX1), *SLC9A3,* etc.	Yes
	6.	GO:0015075	Ion transmembrane transporter activity	106/451	4.28E−07	*CLCA2, ATP12A, CACNA2D3, KCNJ15, SLC15A2, SLC8A1,* (P2RX1), *SLC9A3, KCNC4, SLC5A5,* etc.	Yes
	7.	GO:0015318	Inorganic molecular entity transmembrane transporter activity	99/413	4.28E−07	*CLCA2, RBP4, ATP12A, CACNA2D3, KCNJ15, SLC15A2, SLC8A1,* (P2RX1), *SLC9A3, KCNC4,* etc.	Yes
	8.	GO:0005509	Calcium ion binding	79/316	2.34E−06	*ADGRL3, SCUBE2, FBN2,* (SCIN), (HPCAL4), *CCBE1,* (CASR), *DLL1,* (CDK5R1), (TBC1D9), etc.	Yes
	9.	GO:0022836	Gated channel activity	40/135	9.99E−05	*CLCA2, CACNA2D3, KCNJ15,* (P2RX1), *KCNC4,* (KCNAB2), (GABRD), *KCNA6,* (ANO1), *KCNJ2,* etc.	Yes
	10.	GO:0046873	Metal ion transmembrane transporter activity	54/208	1.20E−04	*ATP12A, CACNA2D3, KCNJ15, SLC8A1, SLC9A3, KCNC4, SLC5A5,* (KCNAB2), *SLC4A9, SLC6A19,* etc.	Yes
T versus S	1.	GO:0038023	Signaling receptor activity	106/342	4.11E−08	*ADGRL3, PPARG, TDGF1, PTGER4, NPSR1, BMPR1B,* (P2RX1), *LPAR3, NOTCH3,* (GABBR2), etc.	Yes
	2.	GO:0004888	Transmembrane signaling receptor activity	84/256	1.13E−07	*ADGRL3, PTGER4, NPSR1, BMPR1B,* (P2RX1), *LPAR3,* (GABBR2), *MFSD6, SORT1,* (TRPA1), etc.	Yes
	3.	GO:0060089	Molecular transducer activity	111/386	6.85E−07	*ADGRL3, PPARG, TDGF1, PTGER4, NPSR1, BMPR1B,* (P2RX1), *LPAR3, NOTCH3,* (GABBR2), etc.	Yes
	4.	GO:0005215	Transporter activity	155/603	2.11E−06	*SLC27A6, ATP12A, RBP4, KCNJ15, CACNA2D3, STAR, SLC7A11, ABCA12, UCP2, SLC15A2,* etc.	Yes
	5.	GO:0015075	Ion transmembrane transporter activity	120/442	3.82E−06	*ATP12A, KCNJ15, CACNA2D3, SLC7A11, SLC15A2, SLC5A5, SLC8A1, SLC26A3,* (P2RX1), *SCN11A,* etc.	Yes
	6.	GO:0015318	Inorganic molecular entity transmembrane transporter activity	110/405	1.30E−05	*ATP12A, RBP4, KCNJ15, CACNA2D3, SLC7A11, SLC15A2, SLC5A5, SLC8A1, SLC26A3,* (P2RX1), etc.	Yes

(Continues)

TABLE 7 (Continued)

Contrast	GO ID	Molecular Function (MF)	DE/All Genes	p-value	MF DEGs (Highest $|\log_2FC|$)[a]	MF sig. in both O versus S/T versus S?
7.	GO:0022857	Transmembrane transporter activity	136/533	1.82E−05	ATP12A, RBP4, KCNJ15, CACNA2D3, SLC7A11, ABCA12, UCP2, SLC15A2, SLC5A5, SLC8A1, etc.	Yes
8.	GO:0005509	Calcium ion binding	87/306	3.08E−05	ADGRL3, FBN2, (SCIN), CCBE1, NOTCH3, PLCB1, TPD52, (CASR), MYL9, CLSTN1, etc.	Yes
9.	GO:0008289	Lipid binding	119/465	8.22E−05	GSDMA, HSD11B2, RBP4, PPARG, STAR, BSPRY, APOB, PXDC1, SNX31, LPAR3, etc.	Yes
10.	GO:0005102	Signaling receptor binding	202/892	1.67E−04	IL1B, TGFB3, IFNG, CXCL12, PPARG, LPIN1, ABCA12, PDPN, TDGF1, MAGI2, etc.	Yes

Abbreviations: O, distinct ovoid; S, distinct spherical; T, distinct tubular.

[a]MF DEGs are listed in order of highest to lowest $|\log_2FC|$; DEGs in bold = upregulated; DEGs within parentheses = downregulated; only the 10 DEGs with highest $|\log_2FC|$ are listed for each MF, followed by etc.

to O morphology and S to T morphology (Figure 5; Table S4). Phospholipase A2 (PLA2) group XIIB (*PLA2G12B*), PLA2 group VII (*PLA2G7*), and PLA2 group XVI (*PLA2G16* or *PLAAT3*) were significantly upregulated from S to O and/or S to T conceptus morphologies, similar to a previously reported increase in porcine conceptus PLA2 expression and activity during elongation (Davis et al., 1983). During preimplantation development, the porcine conceptus undergoes remodeling of the lipid composition within the trophoblast phospholipid membrane, including PLA2-stimulated release of arachidonic acid (AA), to allow for trophectoderm cell motility that is essential to rapid conceptus elongation (Geisert et al., 2017). In addition to increasing fluidity of the trophoblast membrane, free AA can serve as precursors for bioactive signaling lipids and phospholipids during membrane remodeling (Geisert et al., 2014; Hanna & Hafez, 2018). In the current study, several genes involved in phospholipid and glycerophospholipid metabolism (Figure 5b) (Kumari et al., 2012; Prasad et al., 2011; Shulga et al., 2011; C. L. E. Yen et al., 2002), phosphatidylcholine and phosphatidylethanolamine metabolism (Figure 5c) (Cao et al., 2008; Golczak et al., 2012; Horibata & Hirabayashi, 2007; Payton et al., 2004; Schaloske & Dennis, 2006; Tsuboi et al., 2015), and the metabolism of membrane sphingolipids (Figure 5d) (T. J. Kim et al., 2006; Lahiri et al., 2007; Tafesse et al., 2007; Takahashi & Suzuki, 2012; Xu et al., 2006) were significantly differentially expressed between 1st MT conceptus stages and T versus S morphologies. Previous studies have observed an increase in proteins involved in the metabolism of ceramide and other membrane sphingolipids, as well as in glycerophospholipid and sphingolipid metabolites, within uterine luminal fluid at the time of porcine conceptus elongation (Kayser et al., 2006; Walsh et al., 2020), providing further support for involvement of phospholipid membrane compositional changes in the initiation of porcine conceptus elongation. In addition to regulating cell maintenance and growth, membrane phospholipids play important roles in regulating membrane−associated protein activities and serve as precursors of bioactive lipids involved in intracellular signaling (Cao et al., 2008; Shulga et al., 2011; Tafesse et al., 2007; Takahashi & Suzuki, 2012). Taken together, the results highlighted above identify specific PLA2 genes that potentially act as stimulators of the porcine conceptus trophectoderm membrane remodeling that is fundamental to the initiation of elongation, which may also involve changes in glycerophospholipid and sphingolipid composition.

The preimplantation period of porcine conceptus development is also associated with significant changes in various aspects of lipid metabolism that are involved in lipid molecular signaling within the uterine environment, including altered lipid uptake, activation, and modification, and biosynthesis of lipid signaling molecules (Blitek & Szymanska, 2017). In the current study, many of the significant DEGs and pathways between conceptus stages within the 1st MT and OMT reflect lipid metabolic changes involved in lipid signaling during the initiation of porcine conceptus elongation (Figure 5; Table S4). Arachidonate 12-lipoxygenase, 12S-type (*ALOX12*), encoding an enzyme that converts AA released from membrane phospholipids into bioactive lipid precursors (Zheng et al., 2020), was significantly

TABLE 8 Significant DEGs ($p \leq 0.05$ and $|\log_2 FC| \geq 1$) between T versus O conceptus morphologies during the initiation of elongation

FC Direction		DEG Symbol	Entrez ID	$\log_2 FC$	p-value
Upregulated	1.	**LY6G6C**	68468	2.56	1.23E−02
	2.	**RAB31**	106572	1.23	7.06E−03
Downregulated	1.	(SFRP1)	20377	−2.21	5.32E−04
	2.	(SYNPO2)	118449	−1.90	1.17E−02
	3.	(LPL)	16956	−1.72	2.72E−02
	4.	(RALGDS)	19730	−1.72	1.17E−02
	5.	(PDE3B)	18576	−1.68	4.49E−02
	6.	(PKD2)	18764	−1.42	1.53E−02
	7.	(RHBDL3)	246104	−1.37	1.26E−02
	8.	(LOC102164598)		−1.33	4.62E−02
	9.	(MAN1C1)	230815	−1.27	2.72E−02
	10.	(PKDCC)	106522	−1.11	2.72E−02
	11.	(ARID5B)		−1.05	1.23E−02
	12.	(PIK3AP1)		−1.03	2.72E−02
	13.	(LOC100620238)		−1.03	1.17E−02

Abbreviations: O, distinct ovoid; T, distinct tubular.

TABLE 9 Significantly enriched biological processes and molecular functions ($p \leq 0.05$) between T versus O conceptus morphologies during the initiation of elongation

GO Analysis		GO ID	GO Term	DE/All Genes	p-value	Term DEGs[a]
Biological Process	1.	GO:0071417	Cellular response to organonitrogen compound	5/327	2.77E−02	(SFRP1), (LPL), (PDE3B), (PKD2), **RAB31**
	2.	GO:1901699	Cellular response to nitrogen compound	5/364	2.77E−02	(SFRP1), (LPL), (PDE3B), (PKD2), **RAB31**
Molecular Function	1.	GO:0051371	Muscle alpha-actinin binding	2/13	1.82E−02	(SYNPO2), (PKD2)
	2.	GO:0005509	Calcium ion binding	4/306	2.20E−02	(LPL), (PKD2), (RHBDL3), (MAN1C1)
	3.	GO:0051393	Alpha-actinin binding	2/22	2.20E−02	(SYNPO2), (PKD2)
	4.	GO:0042805	Actinin binding	2/29	2.31E−02	(SYNPO2), (PKD2)
	5.	GO:0048763	Calcium-induced calcium release activity	1/1	3.38E−02	(PKD2)
	5.	GO:0017129	Triglyceride binding	1/1	3.38E−02	(LPL)

Abbreviations: O, distinct ovoid; T, distinct tubular.
[a]GO term DEGs are listed in order of highest to lowest $|\log_2 FC|$; DEGs in bold = upregulated; DEGs within parentheses = downregulated

upregulated from S to O conceptus morphologies, specifically from O_{T1} to O, and from S to T. The principal product resulting from ALOX12 catalysis of AA is the lipid signaling molecule 12(S)-hydroxyeicosatetraenoic acid (12S-HETE) that has been shown to promote cell survival, migration, and angiogenesis (W. S. Powell & Rokach, 2015), all of which play essential roles in elongation of the porcine conceptus. Another mechanism of lipid signaling within the uterine environment during porcine pregnancy is through glucocorticoids, including cortisol. In the current study, hydroxysteroid 11-beta dehydrogenase 2 (HSD11B2), encoding an enzyme that generates inactive cortisone from active cortisol (Simmons

et al., 2010), was significantly upregulated from S to O conceptus morphologies, specifically from S to S_{T1}, and from S to T. Cortisol has been implicated as an important regulator of conceptus elongation in sheep and cattle via binding and activation of the glucocorticoid receptor (GR) in the maternal endometrium (Dorniak et al., 2013). GR (or NR3C1) is also expressed in the conceptus, as glucocorticoids play a role in a number of important processes during development (Brooks et al., 2015). It has been hypothesized that conceptus expression of HSD11B2 functions to protect the conceptus from the abundance of uterine luminal cortisol that regulates endometrial expression of genes essential to elongation (Brooks et al., 2015;

TABLE 10 Numbers of significant DEGs, pathways, and GO terms between blastocysts at specific sequential stages of development (S_{T1} vs. S, O_{T1} vs. S_{T1}, O vs. O_{T1}, O_{T2} vs. O, T_{T2} vs. O_{T2}, and T vs. T_{T2}) throughout the initiation of elongation

ANALYSIS		1st Morphological Transition (1st MT) (S to O)					2nd Morphological Transition (2nd MT) (O to T)			
		S_{T1} versus S	O_{T1} versus S_{T1}	O versus O_{T1}	1st MT Total	Both 1st MT/O versus S	O_{T2} versus O	T_{T2} versus O_{T2}	T versus T_{T2}	2nd MT Total
DEGs	Total	101	3	221	311	290	3	4	2	8
Upregulated		**85**	**2**	**118**	**198**	**183**	**0**	**2**	**2**	**4**
Downregulated		(16)	(1)	(103)	(113)	(107)	(3)	(2)	(0)	(5)
Pathways		23	7	1	30	8	5	0	1	5
Biological Processes		92	20	24	129	80	127	37	1	164
Molecular Functions		0	20	10	30	4	12	0	5	12
Cellular Components		10	0	6	11	10	0	0	0	0

Note: DEGs with $p \leq 0.05$ and $|log2FC| \geq 1$ (i.e., FC ≥ 2) and pathways and GO terms with $p \leq 0.05$ were considered statistically significant; DEGs in bold = upregulated; DEGs within parentheses = downregulated.

Abbreviations: O, distinct ovoid; OT1, transitional ovoid during the first morphological transition; OT2, transitional ovoid during the second morphological transition; S, distinct spherical; ST1, transitional spherical; TT2, transitional tubular; T, distinct tubular.

Simmons et al., 2010). Additionally, long-chain fatty acid transport protein (FATP) 6 (*SLC27A6*) was significantly upregulated from S to O morphology, specifically from S_{T1} to O_{T1} within the PPAR signaling pathway, and from S to T within the current study. This gene encodes a protein critical in the uptake of fatty acids, including AA (M. C. Yen et al., 2019), for lipid metabolism, such as synthesis of membrane and bioactive signaling lipids (Ribeiro et al., 2016). A major mechanism of lipid signaling is through activation of peroxisome proliferator-activated receptors (PPARs) that have been implicated as essential regulators of conceptus elongation in pigs and ruminants (Blitek & Szymanska, 2017). The FATP gene *SLC27A6* has been shown to increase during bovine conceptus elongation in conjunction with *PPAR* expression (Ribeiro et al., 2016), similar to the increased *PPAR* expression occurring in the elongating ovine and porcine conceptus (Blitek & Szymanska, 2017). In the current study, PPAR gamma (*PPARG*) was significantly upregulated from S to O conceptus morphologies, specifically from O_{T1} to O, and from S to T. Collectively, the upregulation of *ALOX12*, *HSD11B2*, *SLC27A6*, and *PPARG* throughout the S to O and S to T transitions within the current study further validates the vital role of lipid signaling in establishing a uterine environment that promotes conceptus survival, development, and successful elongation, and implicates the regulation of these specific genes as instrumental to the initiation of porcine conceptus elongation.

3.3 | ECM remodeling and cellular adhesion

In the current study, multiple significant DEGs and pathways between conceptus stages throughout the 1st MT and across the OMT are related to ECM remodeling and cellular adhesion (Figure 6; Table S4). During the peri-implantation period, the porcine conceptus trophectoderm undergoes reorganization of the ECM to facilitate adhesion between the conceptus and uterine epithelium, which is essential for the trophectoderm cell migration that occurs during

rapid elongation (Erikson et al., 2009). It has been proposed that initial attachment of the conceptus to the luminal epithelium involves low-affinity contacts, such as carbohydrate ligand-lectin receptor binding, which are then replaced by more stable adhesions involving ECM molecules and integrins to promote conceptus elongation and implantation (Bazer et al., 2010; Erikson et al., 2009; Geisert et al., 2015). Within the current study, galactoside alpha-(1,2)-fucosyltransferase 1 (*FUT1*), encoding an enzyme that catalyzes formation of the H type 1 antigen (J. K. Powell et al., 2000), was significantly downregulated from S to O, specifically from S to S_{T1} and O_{T1} to O, and from S to T. It has been suggested that the H type 1 antigen may function as a carbohydrate ligand in initial low-affinity contacts established between trophectoderm and endometrium at the initiation of the adhesion cascade (Bowen & Burghardt, 2000; Geisert et al., 2015). Therefore, downregulation of *FUT1* throughout the initial stages of elongation may be due to the decreasing utilization of this low-affinity adhesion mechanism as the conceptus begins to more firmly attach to the endometrium through the actions of integrins and ECM molecules, such as fibronectin, laminin, secreted phosphoprotein 1 (SPP1), and hyaluronan (HA) (Ashworth et al., 2010; Ziecik et al., 2011), to promote morphological change. Within the current study, HA synthase 2 (*SHAS2*) and *HAS1*, encoding trans-membrane enzymes that synthesize HA (Raheem, 2018), and cluster domain 44 (*CD44*), encoding the principal cell surface receptor for HA (Stojkovic et al., 2003), were significantly upregulated from S to O, with *SHAS2* and *CD44* specifically upregulated from O_{T1} to O and from S to T blastocysts. HA-CD44 binding has been hypothesized to act as a bridge between the conceptus and uterine epithelium (Berneau et al., 2019), and additional molecules present at the maternal-conceptus interface at the time of conceptus attachment may associate with this CD44-anchored HA (Ashworth et al., 2010), serving to stabilize the ECM and allow for firm attachments to potentially drive conceptus elongation and implantation (Erikson et al., 2009; Hettinger et al., 2001; Ross et al., 2003). Finally, cell

TABLE 11 Ten most highly upregulated significant DEGs ($p \leq 0.05$ and $|log_2FC| \geq 1$) between blastocysts at sequential stages of development (S_{T1} vs. S, O_{T1} vs. S_{T1}, and O vs. O_{T1}) throughout the first morphological transition during the initiation of elongation

Contrast		DEG Symbol	Entrez ID	log_2FC	p-value	Associated Significantly Enriched Pathways ($p \leq .05$)	DEG upregulated in O versus S?
S_{T1} versus S	1.	*IFNG*	15978	6.98	2.09E−06	Cytokine–cytokine receptor interaction; Th1 and Th2 cell differentiation; Graft-versus-host disease; Th17 cell differentiation; TGF-beta signaling pathway; Necroptosis; Antigen processing and presentation; HIF-1 signaling pathway	Yes
	2.	*IL1B*	16176	6.49	1.34E−02	Cytokine–cytokine receptor interaction; MAPK signaling pathway; Graft-versus-host disease; Th17 cell differentiation; NF-kappa B signaling pathway; Necroptosis	Yes
	3.	*LOC110258125*		5.76	2.82E−02	N/A	Yes
	4.	*LOC110255300*		5.42	3.28E−05	N/A	Yes
	5.	*IL1B2*		5.30	3.28E−05	N/A	Yes
	6.	*LOC110258095*		5.14	9.90E−05	N/A	Yes
	7.	*LOC110258578*		4.83	1.17E−04	N/A	Yes
	8.	*LOC110258582*		4.83	6.13E−05	N/A	Yes
	9.	*RBP4*	19662	3.97	2.77E−03	X	Yes
	10.	*LOC110259156*		3.91	2.09E−03	N/A	Yes
O_{T1} versus S_{T1}	1.	*SLC27A6*	225579	5.14	3.53E−04	PPAR signaling pathway	Yes
	2.	*CYP17A1*	13074	4.89	6.39E−03	Steroid hormone biosynthesis; Ovarian steroidogenesis; Cortisol synthesis and secretion; Prolactin signaling pathway	Yes
O versus O_{T1}	1.	*RN18S*	19791	4.87	3.18E−02	X	Yes
	2.	*LOC106505418*		4.30	1.90E−03	N/A	Yes
	3.	*FRY*	320365	3.52	9.60E−04	X	Yes
	4.	*LOC110255743*		3.26	2.61E−02	N/A	Yes
	5.	*LOC102158335*		3.05	1.67E−02	N/A	Yes
	6.	*ALOX12*	11684	2.99	1.21E−02	X	Yes
	7.	*TGFB3*	21809	2.93	1.67E−02	X	Yes
	8.	*TF*	21779	2.54	2.53E−02	X	No
	9.	*LOC110261996*		2.47	2.48E−02	N/A	Yes
	10.	*IGFBP3*	16009	2.33	3.82E−02	X	Yes

Abbreviations: OT1, transitional ovoid during the first morphological transition; O, distinct ovoid; S, distinct spherical; ST1, transitional spherical.

migration-inducing hyaluronidase 1 (*CEMIP*), encoding an HA-binding protein with HA-degradation capability (Nagaoka et al., 2015), was significantly downregulated from S to O, specifically from O_{T1} to O, and from S to T in the current study, potentially indicating reduced degradation of HA and maintenance of ECM stability as the adhesion cascade proceeds and the abundance of low-affinity contacts continues to decrease throughout the initiation of porcine conceptus elongation.

Further indication of increasing stability of trophectoderm-endometrial attachments throughout the initiation of porcine conceptus elongation was the significant upregulation of genes forming fibronectin and laminin ECM proteins, as well as several integrin subunits, from S to O and S to T conceptus morphologies within the current study. This

increased expression of integrin subunits is consistent with a recently reported upregulation of several of these integrin subunits by the porcine conceptus over the elongation period (Zeng et al., 2019). During porcine conceptus elongation, both the soluble ECM adhesion protein SPP1 and expression of integrin subunits for the SPP1 receptor are present at the maternal-conceptus interface (Erikson et al., 2009; Garlow et al., 2002). It is hypothesized that binding of the Arg-Gly-Asp (RGD) sequence of porcine SPP1 to integrins on both the uterine epithelium and conceptus trophectoderm facilitates trophectoderm attachment, spreading, and migration during conceptus elongation via adhesion at the maternal-conceptus interface (Erikson et al., 2009; Garlow et al., 2002). Furthermore, covalent conjugation of the RGD peptide to an alginate matrix

TABLE 12 Ten most highly downregulated significant DEGs ($p \leq 0.05$ and $|log_2FC| \geq 1$) between blastocysts at sequential stages of development (S_{T1} vs. S, O_{T1} vs. S_{T1}, and O vs. O_{T1}) throughout the first morphological transition during the initiation of elongation

Contrast		DEG Symbol	Entrez ID	log_2FC	p-value	Associated Significantly Enriched Pathways ($p \leq 0.05$)	DEG downregulated in O versus S?
S_{T1} versus S	1.	(KCNA1)	16485	−3.00	1.21E−02	X	No
	2.	(SCIN)	20259	−2.57	9.96E−03	X	Yes
	3.	(KRBA1)	77827	−1.88	9.90E−05	X	Yes
	4.	(FUT1)	14343	−1.80	9.81E−03	X	Yes
	5.	(SOX21)	223227	−1.55	6.42E−03	X	Yes
	6.	(ZNF146)	26465	−1.33	4.26E−03	X	No
	7.	(TRIM50)	215061	−1.22	6.42E−03	X	Yes
	8.	(PHEX)	18675	−1.22	2.08E−02	X	Yes
	9.	(ZBTB45)	232879	−1.16	2.46E−02	X	Yes
	10.	(DUSP4)	319520	−1.15	2.57E−03	MAPK signaling pathway	Yes
O_{T1} versus S_{T1}	1.	(LOC110261162)		−3.65	6.47E−07	N/A	No
O versus O_{T1}	1.	(GULO)	268756	−4.33	2.42E−03	X	Yes
	2.	(SERPINE1)	18787	−3.36	1.07E−04	X	Yes
	3.	(CEMIP)	80982	−3.07	4.73E−04	X	Yes
	4.	(ESRRG)	26381	−2.80	1.23E−02	X	Yes
	5.	(DOK7)	231134	−2.76	2.42E−03	X	Yes
	6.	(TRIM15)	69097	−2.48	1.15E−03	X	Yes
	7.	(TRIM10)	19824	−2.47	6.49E−03	X	Yes
	8.	(EPN3)	71889	−2.46	2.42E−03	X	Yes
	9.	(KLHL5)	71778	−2.36	9.48E−04	X	Yes
	10.	(LOC110261490)		−2.35	2.13E−02	N/A	Yes

Abbreviations: OT1, transitional ovoid during the first morphological transition; O, distinct ovoid; S, distinct spherical; ST1, transitional spherical.

encapsulating spherical porcine blastocysts significantly increased the number of blastocysts initiating morphological change in vitro compared to those encapsulated without RGD (Laughlin et al., 2017), providing further evidence for the critical role of RGD-integrin binding in promoting the initiation of porcine conceptus elongation. Lastly, fibronectin and laminin likely function as bridging ligands to promote blastocyst expansion and stable adhesion for uterine receptivity and conceptus implantation (Bazer et al., 2010). Altogether, the results highlighted above indicate the crucial function of ECM and integrin binding within the progressing adhesion cascade during peri-implantation porcine conceptus development and elongation.

4 | MATERIALS AND METHODS

4.1 | Production and collection of blastocysts

All animal protocols were approved by the U.S. Meat Animal Research Center (USMARC) Institutional Animal Care and Use Committee (EO 65.0). Procedures for handling animals complied with the Guide for the Care and Use of Agricultural Animals in Research and Teaching (FASS, 2010). Over a 1-year collection period covering 14 replicate collections of 6 to 10 gilts per replicate, postpubertal White crossbred gilts consisting of Landrace, Yorkshire, and Duroc genetics were checked daily for estrus. Following the first detection of estrus (designated as day 0), gilts ($n = 107$) were artificially inseminated with semen from pooled terminal Duroc sires collected from a commercial boar stud and again 24 h later with the same pool of semen. Semen pools across the 14 replicates sampled different sires within each replicate to remove the influence of individual sires across replicates and treatments. Bred gilts were randomly assigned to gestational day groups (9, 10, or 11) based on estrus detection, and harvested at the USMARC abattoir on their respective day of gestation. Immediately after the gilts had been harvested, their reproductive tracts were removed and each uterine horn was flushed with 20 ml of 25 mM HEPES-buffered RPMI-1640 medium (ThermoFisher Scientific, Waltham, MA; ~37°C) containing 1× antibiotics/antimycotics (Millipore Sigma). From confirmed pregnant gilts ($n = 87$; 81.3% pregnancy rate), all blastocysts were recovered ($n = 1267$) and
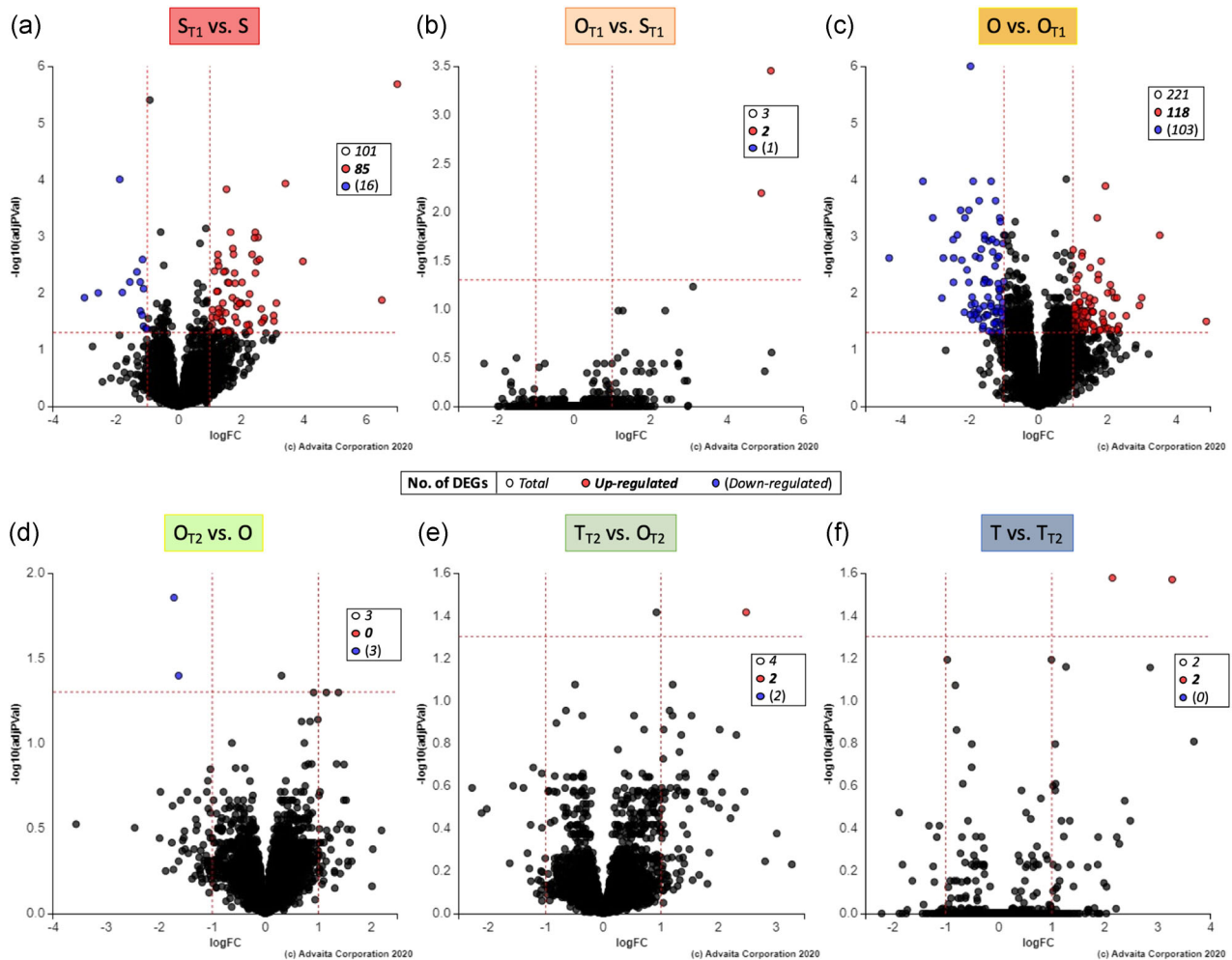
FIGURE 3 Volcano plots of total gene expression changes from (a) distinct S to transitional S_{T1} blastocysts (S_{T1} vs. S), (b) transitional S_{T1} to transitional O_{T1} blastocysts (O_{T1} vs. S_{T1}), (c) transitional O_{T1} to distinct O blastocysts (O vs. O_{T1}), (d) distinct O to transitional O_{T2} blastocysts (O_{T2} vs. O), (e) transitional O_{T2} to transitional T_{T2} blastocysts (T_{T2} vs. O_{T2}), and (f) transitional T_{T2} to distinct T blastocysts (T vs. T_{T2}) throughout the initiation of elongation. Log_2FC (x-axis) against p-value (y-axis) of significant DEGs ($p \leq 0.05$ and $|log_2FC| \geq 1$) upregulated (red) and downregulated (blue). All other DEGs with $p > 0.05$ and/or $|log_2FC| < 1$ are indicated in black. Numbers of significant DEGs between conceptus stages are detailed according to the plot legend within boxes overlayed on corresponding volcano plots

classified into conceptus morphological stages according to morphology and length using a standard stereomicroscope (Nikon Instruments): spherical (0.1–2.5 mm; $n = 404$), ovoid (3–10 mm; $n = 712$), or tubular (12–80 mm; $n = 151$). All recovered blastocysts were individually snap frozen in liquid nitrogen and stored separately at −80°C until selection for RNA-Seq analysis (detailed below). Conceptus populations of each litter were classified according to the uniformity of the most advanced conceptus morphological stage present within the respective litter (i.e., the proportion of all blastocysts within the respective litter that were of the most advanced conceptus morphological stage collected from the litter). Conceptus populations were classified as homogeneous pregnancies when at least 80% of blastocysts within the respective litter were of the most advanced morphological stage present within the litter (due to the difficulty of obtaining 100% homogeneous tubular morphological stage litters), and as heterogeneous pregnancies when less than 80%

of blastocysts within the respective litter were of the most advanced morphological stage present within the litter. Details regarding conceptus variability of these characterized pregnancies for the entire population of harvested gilts are illustrated in Table S5 (upper section). From these homogeneous and heterogeneous pregnancies, individual blastocysts were further selected and sorted into conceptus treatment groups based on the morphological stage of the respective blastocyst and conceptus morphological stage uniformities of the corresponding litter. Figure 1 illustrates the respective conceptus treatment groups as: distinct spherical (S, $n = 8$ blastocysts) from homogeneous spherical stage (100%) pregnancies ($n = 8$ gilts), transitional spherical (S_{T1}, $n = 8$ blastocysts) or transitional ovoid (O_{T1}, $n = 8$ blastocysts) during the first morphological transition from the same heterogeneous spherical (34%)/ovoid (66%) stage pregnancies ($n = 8$ gilts), distinct ovoid (O, $n = 8$ blastocysts) from homogeneous ovoid stage (100%) pregnancies ($n = 8$ gilts), transitional ovoid

TABLE 13 Significantly enriched pathways ($p \leq 0.05$) between blastocysts at sequential stages of development (S_{T1} vs. S, O_{T1} vs. S_{T1}, and O vs. O_{T1}) throughout the first morphological transition during the initiation of elongation

Contrast		Pathway	DE/All Genes	p-value	Pathway DEGs[a]	Pathway sig. in O versus S?
S_{T1} versus S	1.	Cytokine–cytokine receptor interaction	4/80	2.58E−03	**IFNG, IL1B, GDF6, CXCL12**	Yes
	2.	Th1 and Th2 cell differentiation	4/50	5.34E−03	**IFNG, MAML2, NOTCH3, DLL1**	No
	3.	MAPK signaling pathway	4/210	1.51E−02	**IL1B, FGF10**, (DUSP4), **CACNG6**	Yes
	4.	Amoebiasis	3/48	1.51E−02	**IFNG, IL1B**, (ARG1)	Yes
	5.	Graft-versus-host disease	2/4	1.51E−02	**IFNG, IL1B**	No
	6.	Mineral absorption	3/30	1.56E−02	**SLC9A3, SLC26A3, SLC8A1**	No
	7.	Inflammatory bowel disease (IBD)	2/21	1.56E−02	**IFNG, IL1B**	No
	8.	Th17 cell differentiation	2/62	1.56E−02	**IFNG, IL1B**	No
	9.	NF-kappa B signaling pathway	2/66	1.56E−02	**IL1B, CXCL12**	Yes
	10.	TGF-beta signaling pathway	2/69	1.56E−02	**IFNG, GDF6**	No
	11.	Necroptosis	2/90	1.56E−02	**IFNG, IL1B**	No
	12.	Antigen processing and presentation	1/29	1.56E−02	**IFNG**	No
	13.	Protein digestion and absorption	3/39	2.21E−02	**SLC9A3, SLC8A1, MEP1B**	No
	14.	Human cytomegalovirus infection	3/156	2.21E−02	**IL1B, GNG11, CXCL12**	No
	15.	Type I diabetes mellitus	2/7	2.21E−02	**IFNG, IL1B**	Yes
	16.	African trypanosomiasis	2/13	2.21E−02	**IFNG, IL1B**	No
	17.	Salmonella infection	2/55	2.21E−02	**IFNG, IL1B**	No
	18.	Rheumatoid arthritis	3/40	2.52E−02	**IFNG, IL1B, CXCL12**	No
	19.	Steroid hormone biosynthesis	2/13	2.75E−02	**CYP17A1, HSD11B2**	No
	20.	Arginine biosynthesis	2/16	3.83E−02	(ARG1), **ASL**	No
	21.	HIF-1 signaling pathway	2/78	3.83E−02	**IFNG, PFKFB3**	Yes
	22.	Malaria	2/17	4.07E−02	**IFNG, IL1B**	No
	23.	Notch signaling pathway	3/40	4.74E−02	**MAML2, NOTCH3, DLL1**	No
O_{T1} versus S_{T1}	1.	Steroid hormone biosynthesis	1/14	1.33E−02	**CYP17A1**	No
	2.	Ovarian steroidogenesis	1/25	1.33E−02	**CYP17A1**	Yes
	3.	Cortisol synthesis and secretion	1/37	1.33E−02	**CYP17A1**	No
	4.	PPAR signaling pathway	1/44	1.33E−02	**SLC27A6**	No
	5.	Prolactin signaling pathway	1/57	1.67E−02	**CYP17A1**	No
	6.	Insulin resistance	1/84	2.03E−02	**SLC27A6**	No
	7.	Cushing syndrome	1/110	2.88E−02	**CYP17A1**	No
O versus O_{T1}	1.	Cholesterol metabolism	6/34	1.01E−02	**APOB**, (SOAT1), **MYLIP, SORT1, SOAT2**, (NPC1)	Yes

Abbreviations: OT1, transitional ovoid during the first morphological transition; O, distinct ovoid; S, distinct spherical; ST1, transitional spherical.

[a]Pathway DEGs are listed in order of highest to lowest $|\log_2 FC|$; DEGs in bold = upregulated; DEGs within parentheses = downregulated.

(O_{T2}, $n = 8$ blastocysts) or transitional tubular (T_{T2}, $n = 8$ blastocysts) during the second morphological transition from the same heterogeneous ovoid (43%)/tubular (55%) stage pregnancies ($n = 8$ gilts), or distinct tubular (T, $n = 6$ blastocysts) from homogeneous tubular stage

(90%) pregnancies ($n = 6$ gilts). For distinct conceptus treatment groups (i.e., derived from homogeneous pregnancies), one blastocyst was evaluated from each litter, and for transitional conceptus treatment groups (i.e., derived from heterogeneous pregnancies), two total

TABLE 14 Significant DEGs ($p \leq 0.05$ and $|\log_2FC| \geq 1$) between blastocysts at sequential stages of development (O_{T2} vs. O, T_{T2} vs. O_{T2}, and T vs. T_{T2}) throughout the second morphological transition during the initiation of elongation

FC Direction	Contrast		DEG Symbol	Entrez ID	$\log_2FC$	*p*-value	Associated Significantly Enriched Pathways ($p \leq 0.05$)
Upregulated	T_{T2} versus O_{T2}	1.	*FOXA1*	15375	2.48	3.84E−02	X
		2.	*LOC110255743*		1.92	2.09E−02	N/A
	T versus T_{T2}	1.	*TRIM10*	19824	3.27	2.69E−02	X
		2.	*GCNT3*	72077	2.14	2.65E−02	Mucin type O-glycan biosynthesis
Downregulated	O_{T2} versus O	1.	(*LOC106505418*)		−4.81	3.08E−03	N/A
		2.	(*GCNT3*)	72077	−1.72	1.40E−02	Mucin type O-glycan biosynthesis
		3.	(*EGR1*)	13653	−1.64	4.01E−02	GnRH signaling pathway; AGE−RAGE signaling pathway in diabetic complications
	T_{T2} versus O_{T2}	1.	(*LOC110255823*)		−3.69	2.09E−02	N/A
		2.	(*LOC106510322*)		−2.36	3.84E−02	N/A

Abbreviations: O, distinct ovoid; OT2, transitional ovoid during the second morphological transition; T, distinct tubular; TT2, transitional tubular.
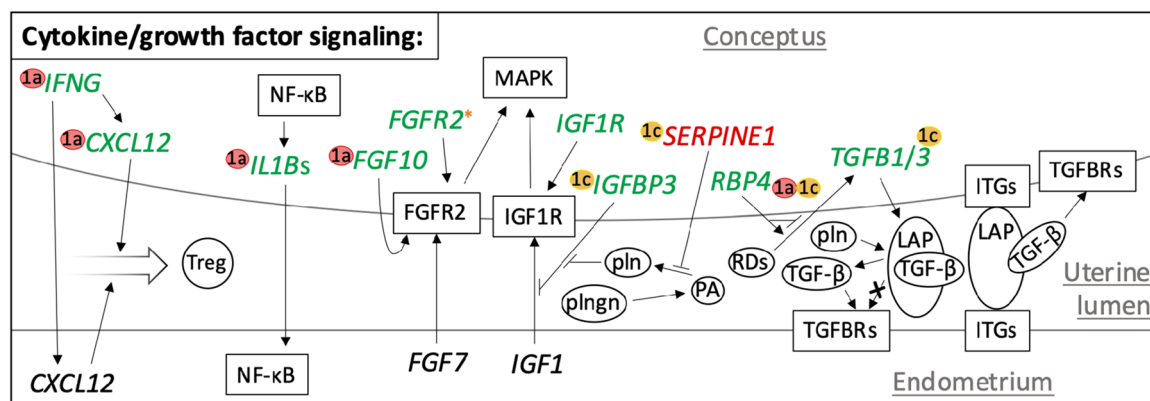
FIGURE 4 Proposed mechanisms of interactions among highlighted significant DEGs throughout the 1st MT from S to O blastocysts (O vs. S) and across the OMT from S to T blastocysts (T vs. S) that indicate differential conceptus regulation of cytokine and growth factor signaling throughout the initiation of elongation. Conceptus IFN-γ can induce expression of *CXCL12* within both the conceptus and endometrium; CXCL12 can recruit Tregs to the maternal-conceptus interface. Conceptus IL1Bs activate NF-κB, which can also induce expression of *IL1Bs*. Endometrial FGF7 and IGF-1, as well as conceptus FGF10, signal through the MAPK pathway by binding to conceptus FGFR2 and IGF1R. Additionally, binding of conceptus IGFBP3 to IGF-1 may inhibit its attachment to IGF1R. Cleavage of IGFBP3 by plasmin to increase IGF-1 bioavailability may be reduced through inhibition of PA plasminogen activation by conceptus SERPINE1. RBP4 may regulate delivery of RDs to the conceptus, which can induce expression of conceptus *TGFBs*. Latent TGF-β complexes secreted by the conceptus can facilitate maternal-conceptus attachment by binding to ITGs on both the endometrium and conceptus. These interactions between latent TGF-β complexes and ITGs may also induce conformational changes in the latent complexes, enabling binding of bioactive TGF-βs to both conceptus and endometrial TGFBRs. Further, PA-activated plasmin is also able to generate bioactive TGF-βs through proteolysis of latent TGF-βs. All highlighted conceptus DEGs were significant between both O versus S and T versus S distinct morphologies unless specifically indicated by an asterisk: orange asterisk = significant between O versus S, while not significant between T versus S. Significant DEGs between blastocysts at sequential stages of development throughout the 1st MT are indicated by bubbles corresponding to specific developmental stage comparisons: 1a = S_{T1} versus S; and 1c = O versus O_{T1}. Green DEGs, upregulated; red DEGs, downregulated; ITGs, integrins; LAP, latency-associated peptide; MAPK, mitogen-activated protein kinase; NF-κB, nuclear factor kappa B; PA, plasminogen activator; pln, plasmin; plngn, plasminogen; RDs, retinoids; TGFBRs, TGF-β receptors; Treg, regulatory T cell

blastocysts were evaluated from each litter (one blastocyst of each morphological stage within the same litter), utilizing RNA-Seq. The primary objective of this study was to evaluate transcriptome differences between conceptus populations (i.e., distinct and transitional) and conceptus morphological stages (i.e., spherical, ovoid, and

tubular) with high temporal resolution; therefore, we did not account for sex of individual blastocysts in this study. Details regarding conceptus variability of the specific population of gilts from which blastocysts were selected for RNA-Seq evaluation are illustrated in Table S5 (lower section).
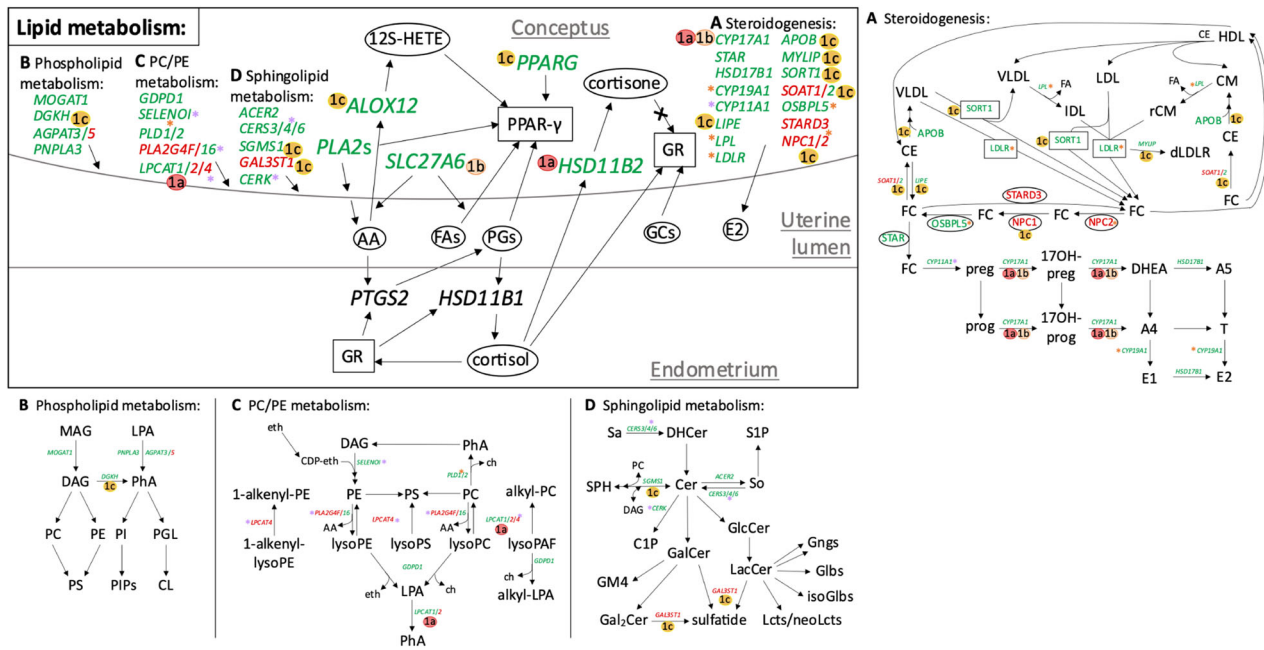
FIGURE 5 Proposed mechanisms of interactions among highlighted significant DEGs throughout the 1st MT from S to O blastocysts (O vs. S) and across the OMT from S to T blastocysts (T vs. S) that indicate differential conceptus regulation of lipid metabolism throughout the initiation of elongation. Differential expression of (a) steroidogenesis-related genes within the conceptus may lead to the increase in synthesis and secretion of E2. PLA2s within the conceptus release AA from phospholipids composing the trophectoderm membrane, which can be utilized for PG synthesis by PTGS2 within the endometrium or for generating 12S-HETE by ALOX12 within the conceptus. Additionally, differential expression of genes involved in (b) phospholipid metabolism, (c) PC/PE metabolism, and (d) sphingolipid metabolism may indicate changes in conceptus phospholipid membrane composition. SLC27A6 facilitates uptake of FAs, including AA, by the conceptus, and PGs, 12S-HETE, AA, and FAs, as well as their derivatives, can bind and activate conceptus PPAR-γ. HSD11B1 generates cortisol in the endometrium, which can bind and activate GR, inducing *PTGS2* expression and upregulation of PG synthesis. Both PGs and activated GR can also induce endometrial *HSD11B1* expression. Endometrial cortisol produced by HSD11B1 as well as GCs can activate conceptus GR; however, conceptus HSD11B2 can covert active cortisol into inactive cortisone, which is unable to bind GR. All highlighted conceptus DEGs were significant between both O versus S and T versus S distinct morphologies unless specifically indicated by an asterisk: orange asterisk = significant between O versus S, while not significant between T versus S; and purple asterisk = significant between T versus S, while not significant between O versus S. Significant DEGs between blastocysts at sequential stages of development throughout the 1st MT are indicated by bubbles corresponding to specific developmental stage comparisons: 1a = S_{T1} versus S; 1b = O_{T1} versus S_{T1}; and 1c = O versus O_{T1}. Green DEGs = upregulated; red DEGs = downregulated; 12S-HETE = 12-hydroxyeicosatetraenoic acid; 17OH-preg = 17-hydroxy-pregnenolone; 17OH-prog = 17-hydroxy-progesterone; A4 = androstenedione; A5 = androstenediol; AA = arachidonic acid; C1P = ceramidE−1-phosphate; CE = cholesteryl ester; Cer = ceramide; ch = choline; CL = cardiolipin; CM = chylomicron; DAG = diacylglycerol; DHCer = dihydroceramide; DHEA = dehydroepiandrosterone; dLDLR = degraded LDLR; E1 = estrone; E2 = estradiol-17β; eth = ethanolamine; FA = fatty acid; FC = free cholesterol; Gal2Cer = galabiosylceramide; GalCer = galactosylceramide; GCs = glucocorticoids; Glbs = globo-series glycosphingolipids; GlcCer = glucosylceramide; GM4 = sialylgalactosylceramide; Gngs = ganglio-series glycosphingolipids; GR = glucocorticoid receptor; HDL = high-density lipoprotein; IDL = intermediatE−density lipoprotein; LacCer = lactosylceramide; Lcts = lacto-series glycosphingolipids; LDL = low-density lipoprotein; LPA = lysophosphatidic acid; MAG = monoacylglycerol; PAF = platelet-activating factor; PC = phosphatidylcholine; PE = phosphatidylethanolamine; PG = prostaglandin; PGL = phosphatidylglycerol; PhA = phosphatidic acid; PI = phosphatidylinositol; PIPs = phosphoinositides; preg = pregnenolone; prog = progesterone; PS = phosphatidylserine; rCM = chylomicron remnant; S1P = sphingosinE−1-phosphate; Sa = sphinganine; So = sphingosine; SPH = sphingomyelin; T = testosterone; VLDL = very low-density lipoprotein

4.2 | RNA isolation, processing, and sequencing

Total RNA was isolated from single spherical, ovoid, and tubular blastocysts using the RNeasy Microkit (Qiagen) with on-column DNase I treatment, as described by the manufacturer. The concentration and quality of the isolated RNA were determined using the Agilent Tapestation 2200 and RNA ScreenTape assay (Agilent Technologies), and only blastocysts within each treatment group having high-quality RNA based on RNA integrity number (RIN) were utilized for RNA-Seq (average RIN of

8.9 with a range of 7.1–10.0). Total RNA was processed and prepared for RNA sequencing with the Illumina TruSeq Stranded Total RNA Library Prep Gold Kit (Illumina, Inc.), and individual conceptus libraries were tagged with TruSeq RNA CD Indexes (Illumina, Inc.) for multiplex sequencing. Library concentrations were confirmed with the Agilent Tapestation 2200 and DNA ScreenTape assay (Agilent Technologies) and Nano-drop One (ThermoFisher Scientific). The libraries were diluted to a final concentration of 4 nM. Libraries were paired-end sequenced with 150 cycle High Output sequencing kits on the NextSeq. 500 Sequencing
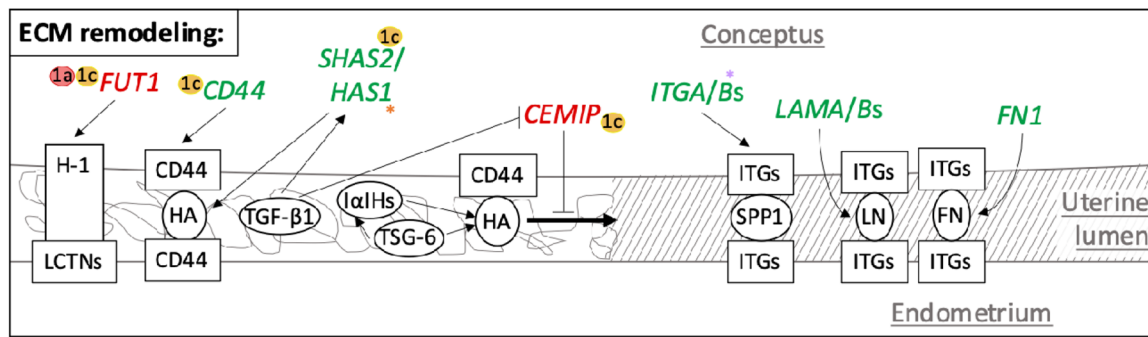
FIGURE 6 Proposed mechanisms of interactions among highlighted significant DEGs throughout the 1st MT from S to O blastocysts (O vs. S) and across the OMT from S to T blastocysts (T vs. S) that indicate differential conceptus regulation of ECM remodeling throughout the initiation of elongation. Conceptus FUT1 may synthesize H-1 to serve as a carbohydrate ligand that binds to LCTNs on the endometrium; these low-affinity contacts may facilitate initial attachment of the conceptus to the uterus. Additionally, interactions between HA and CD44 may act as an initial bridge between conceptus and endometrium. As elongation initiates, conceptus CD44-anchored HA may interact with TSG-6 and IαIHs at the maternal-conceptus interface to stabilize the ECM and allow for more firm attachments between the conceptus and endometrium. TGF-β1 may contribute to this mechanism by inducing conceptus *HAS1* and *SHAS2* expression to up-regulate HA synthesis, as well as by inhibiting conceptus expression of *CEMIP* to reduce HA degradation. Lastly, attachment of SPP1, LN, and FN to ITGs on both the conceptus and endometrium may be essential mechanisms for forming stable adhesions to drive elongation. All highlighted conceptus DEGs were significant between both O versus S and T versus S distinct morphologies unless specifically indicated by an asterisk: orange asterisk = significant between O versus S, while not significant between T versus S; and purple asterisk = significant between T versus S, while not significant between O versus S. Significant DEGs between blastocysts at sequential stages of development throughout the 1st MT are indicated by bubbles corresponding to specific developmental stage comparisons: 1a = S_{T1} versus S; and 1c = O versus O_{T1}. Green DEGs = upregulated; red DEGs = downregulated; FN = fibronectin; H-1 = H type 1 antigen; HA = hyaluronan; ITGs = integrins; IαIHs = inter-alpha-trypsin inhibitor heavy chains; LCTNs = lectin receptors; LN = laminin; SPP1 = secreted phosphoprotein 1; TSG-6 = tumor necrosis factor-alpha-induced protein 6

System (Illumina, Inc.). Corresponding sequence data are available in NCBI Sequence Read Archive under the accession number PRJNA723617.

4.3 | Processing and statistical analysis of RNA-Seq data

The quality of the raw paired-end sequence reads in individual fastq files was assessed using FastQC (Version 0.11.5; www.bioinformatics.babraham.ac.uk/projects/fastqc). Reads were trimmed to remove adapter sequences and low-quality bases (average base quality < 15 in a 4-bp window) using the Trimmomatic software (Version 0.35) (Bolger et al., 2014). The remaining reads were mapped to the Sscrofa 11.1 genome assembly (Genbank Accession GCA_000003025.6) using Hisat2 (Version 2.1.0) (D. Kim et al., 2015), and the NCBI annotation for Sscrofa 11.1 (Release 106) was used to guide the alignment. Stringtie (Pertea et al., 2015) was used to determine read counts for each of the 29,847 genes in the Sscrofa 11.1 reference annotation (Release 106). For each comparison, genes with low read counts, <15 reads in at least eight samples, were filtered out. DEGs were identified using DESeq. 2 (Love et al., 2014). An FDR-corrected $p ≤ 0.05$ and $|log_2$ fold change$| ≥ 1$ (i.e., fold change ≥ 2) between treatments was considered statistically significant.

4.4 | GO enrichment and pathway analysis

Enrichment analysis of gene function and cellular pathways was performed using the iPathwayGuide software (Version 1910; Advaita Bio, http://advaitabio.com/ipathwayguide) with the default *Mus musculus* data as background. For GO analysis, an over-representation test, based on a hypergeometric distribution, was used to compute the statistical significance of observing more than the expected number of DEGs. A GO term was considered statistically significant at FDR-corrected $p ≤ 0.05$. Pathway over-representation analysis was performed by comparing the number of affected genes associated with a pathway between groups. Pathways were considered statistically significant at FDR-corrected $p ≤ 0.05$. When selecting DEGs to discuss in this manuscript, further filtering was performed based on the pathways identified as significantly enriched from the DEG data, the fold change values of DEGs identified as significant within a given comparison, overlap of significant DEGs between the distinct morphology (O vs. S, T vs. O, and T vs. S) and specific developmental stage (S_{T1} vs. S, O_{T1} vs. S_{T1}, O vs. O_{T1}, O_{T2} vs. O, T_{T2} vs. O_{T2}, and T vs. T_{T2}) comparisons, and relevance of function in terms of plausible potential mechanisms contributing to elongation during this period of development.

5 | CONCLUSION

The results of this study highlight extensive differences in gene expression between distinct S, O, and T porcine conceptus morphologies, as well as changes in gene expression as the porcine conceptus transitions through specific developmental stages amidst these distinct morphologies, during the initiation of elongation. In particular, the high quantity and fold change of significant DEGs and pathways throughout the spherical to ovoid transition observed in this study, as opposed to minimal changes from ovoid to tubular, suggest that this 1st MT may be most critical to the initiation of elongation. Further, identification of significant DEGs between specific sequential stages of development throughout the 1st MT provided select gene expression profiles with higher temporal resolution, identifying specific DEGs with substantial and rapid changes in expression that may be crucial to the initiation of porcine conceptus elongation. Altogether, these results illustrate extensive DEG coverage of known elongation signaling pathways, implicate conceptus regulation of phospholipid membrane remodeling and lipid molecular signaling as potential key elongation mechanisms, and suggest that the adhesion cascade involving ECM remodeling that occurs throughout the peri-implantation period may begin during the initiation of elongation. Overall, the information gained from this study can be used to further elucidate mechanisms essential to the successful initiation of elongation as the porcine conceptus transitions between specific developmental stages and distinct morphologies, advancing knowledge of porcine conceptus elongation and development to improve swine reproductive outcomes.

CONFLICT OF INTERESTS

The authors declare that there are no conflict of interests.

DATA AVAILABILITY STATEMENT

The data that support the findings of this study are openly available in NCBI Sequence Read Archive at https://www.ncbi.nlm.nih.gov/bioproject/PRJNA723617/, reference number PRJNA723617; additionally, the data that support the findings of this study are available in the supplementary material of this article.

ORCID

Jeremy R. Miles http://orcid.org/0000-0003-4765-8400
Lea A. Rempel https://orcid.org/0000-0002-8344-5085
Angela K. Pannier https://orcid.org/0000-0002-7589-9351

REFERENCES

Ashworth, M. D., Ross, J. W., Stein, D., White, F., & Geisert, R. D. (2010). Endometrial gene expression of acute phase extracellular matrix components following estrogen disruption of pregnancy in pigs. *Animal Reproduction Science*, 122(3–4), 215–221. https://doi.org/10.1016/j.anireprosci.2010.08.013

Bazer, F. W., Geisert, R. D., Thatcher, W. W., & Roberts, R. M. (1982). The establishment and maintenance of pregnancy. In (Eds.) Cole, D. J. A. & Foxcroft, G. R., *Control of pig reproduction* (pp. 227–252). London, England: Butterworth Scientific.

Bazer, F. W., & Johnson, G. A. (2014). Pig blastocyst-uterine interactions. *Differentiation*, 87(1–2), 52–65. https://doi.org/10.1016/j.diff.2013.11.005

Bazer, F. W., Thatcher, W. W., Martinat-Botte, F., & Terqui, M. (1988). Conceptus development in Large White and prolific Chinese Meishan pigs. *Journal of Reproduction and Fertility*, 84(1), 37–42. https://doi.org/10.1530/jrf.0.0840037

Bazer, F. W., Wu, G., Spencer, T. E., Johnson, G. A., Burghardt, R. C., & Bayless, K. (2010). Novel pathways for implantation and establishment and maintenance of pregnancy in mammals. *Molecular Human Reproduction*, 16(3), 135–152. https://doi.org/10.1093/molehr/gap095

Berneau, S. C., Ruane, P. T., Brison, D. R., Kimber, S. J., Westwood, M., & Aplin, J. D. (2019). Investigating the role of CD44 and hyaluronate in embryo-epithelial interaction using an in vitro model. *Molecular Human Reproduction*, 25(5), 265–273. https://doi.org/10.1093/molehr/gaz011

Blitek, A., & Szymanska, M. (2017). Peroxisome proliferator-activated receptor (PPAR) isoforms are differentially expressed in peri-implantation porcine conceptuses. *Theriogenology*, 101, 53–61. https://doi.org/10.1016/j.theriogenology.2017.06.013

Blomberg, L. A., Garrett, W. M., Guillomot, M., Miles, J. R., Sonstegard, T. S., Van Tassell, C. P., & Zuelke, K. A. (2006). Transcriptome profiling of the tubular porcine conceptus identifies the differential regulation of growth and developmentally associated genes. *Molecular Reproduction and Development*, 73(12), 1491–1502. https://doi.org/10.1002/mrd.20503

Blomberg, L. A., Long, E. L., Sonstegard, T. S., Van Tassell, C. P., Dobrinsky, J. R., & Zuelke, K. A. (2005). Serial analysis of gene expression during elongation of the peri-implantation porcine trophectoderm (conceptus). *Physiological Genomics*, 20(2), 188–194. https://doi.org/10.1152/physiolgenomics.00157.2004

Bolger, A. M., Lohse, M., & Usadel, B. (2014). Trimmomatic: A flexible trimmer for Illumina sequence data. *Bioinformatics*, 30(15), 2114–2120. https://doi.org/10.1093/bioinformatics/btu170

Bowen, J. A., & Burghardt, R. C. (2000). Cellular mechanisms of implantation in domestic farm animals. *Seminars in Cell and Developmental Biology*, 11(2), 93–104. https://doi.org/10.1006/scdb.2000.0155

Brooks, K., Burns, G., & Spencer, T. E. (2015). Biological roles of hydroxysteroid (11-beta) dehydrogenase 1 (HSD11B1), HSD11B2, and glucocorticoid receptor (NR3C1) in sheep conceptus elongation. *Biology of Reproduction*, 93(2), 38. https://doi.org/10.1095/biolreprod.115.130757

Cao, J., Shan, D., Revett, T., Li, D., Wu, L., Liu, W., Tobin, J. F., & Gimeno, R. E. (2008). Molecular identification of a novel mammalian brain isoform of acyl-CoA:lysophospholipid acyltransferase with prominent ethanolamine lysophospholipid acylating activity, LPEAT2. *Journal of Biological Chemistry*, 283(27), 19049–19057. https://doi.org/10.1074/jbc.M800364200

Chang, W. C., Huang, S. F., Lee, Y. M., Lai, H. C., Cheng, B. H., Cheng, W. C., Ho, J. Y. P., Jeng, L. B., & Ma, W. L. (2017). Cholesterol import and steroidogenesis are biosignatures for gastric cancer patient survival. *Oncotarget*, 8(1), 692–704. https://doi.org/10.18632/oncotarget.13524

Davis, D. L., Pakrasi, P. L., & Dey, S. K. (1983). Prostaglandins in swine blastocysts. *Biology of Reproduction*, 28(5), 1114–1118. https://doi.org/10.1095/biolreprod28.5.1114

Dorniak, P., Welsh, T. H., Bazer, F. W., & Spencer, T. E. (2013). Cortisol and interferon tau regulation of endometrial function and conceptus development in female sheep. *Endocrinology*, 154(2), 931–941. https://doi.org/10.1210/en.2012-1909

Du, X., Kumar, J., Ferguson, C., Schulz, T. A., Ong, Y. S., Hong, W., Prinz, W. A., Parton, R. G., Brown, A. J., & Yang, H. (2011). A role for oxysterol-binding protein-related protein 5 in endosomal cholesterol trafficking. *Journal of Cell Biology*, 192(1), 121–135. https://doi.org/10.1083/jcb.201004142

Erikson, D. W., Burghardt, R. C., Bayless, K. J., & Johnson, G. A. (2009). Secreted phosphoprotein 1 (SPP1, osteopontin) binds to integrin alpha v beta 6 on porcine trophectoderm cells and integrin alpha v beta 3 on uterine luminal epithelial cells, and promotes trophectoderm cell adhesion and migration. *Biology of Reproduction*, 81(5), 814–825. https://doi.org/10.1095/biolreprod.109.078600

FASS. (2010). *Guide for care and use of agricultural animals in research and teaching* (3rd ed.). Federation of Animal Science Societies.

Garlow, J. E., Ka, H., Johnson, G. A., Burghardt, R. C., Jaeger, L. A., & Bazer, F. W. (2002). Analysis of osteopontin at the maternal-placental interface in pigs. *Biology of Reproduction*, 66(3), 718–725. https://doi.org/10.1095/biolreprod66.3.718

Geisert, R. D., Chamberlain, C. S., Vonnahme, K. A., Malayer, J. R., & Spicer, L. J. (2001). Possible role of kallikrein in proteolysis of insulin-like growth factor binding proteins during the oestrous cycle and early pregnancy in pigs. *Reproduction*, 121(5), 719–728. https://doi.org/10.1530/rep.0.1210719

Geisert, R. D., Johnson, G. A., & Burghardt, R. C. (2015). Implantation and establishment of pregnancy in the pig. *Advances in Anatomy, Embryology and Cell Biology*, 216, 137–163. https://doi.org/10.1007/978-3-319-15856-3_8

Geisert, R. D., Lucy, M. C., Whyte, J. J., Ross, J. W., & Mathew, D. J. (2014). Cytokines from the pig conceptus: Roles in conceptus development in pigs. *Journal of Animal Science and Biotechnology*, 5, 51. https://doi.org/10.1186/2049-1891-5-51

Geisert, R. D., Renegar, R. H., Thatcher, W. W., Roberts, R. M., & Bazer, F. W. (1982). Establishment of pregnancy in the pig: I. Interrelationships between preimplantation development of the pig blastocyst and uterine endometrial secretions. *Biology of Reproduction*, 27(4), 925–939. https://doi.org/10.1095/biolreprod27.4.925

Geisert, R. D., Whyte, J. J., Meyer, A. E., Matthew, D. J., Juarez, M. R., Lucy, M. C., Prather, R. S., & Spencer, T. E. (2017). Rapid conceptus elongation in the pig: An interleukin 1 beta 2 and estrogen-regulated phenomenon. *Molecular Reproduction and Development*, 84(9), 760–774. https://doi.org/10.1002/mrd.22813

Golczak, M., Kiser, P. D., Sears, A. E., Lodowski, D. T., Blaner, W. S., & Palczewski, K. (2012). Structural basis for the acyltransferase activity of lecithin:retinol acyltransferase-like proteins. *Journal of Biological Chemistry*, 287(28), 23790–23807. https://doi.org/10.1074/jbc.M112.361550

Green, M. L., Simmen, R. C., & Simmen, F. A. (1995). Developmental regulation of steroidogenic enzyme gene expression in the periimplantation porcine conceptus: a paracrine role for insulin-like growth factor-I. *Endocrinology*, 136(9), 3961–3970. https://doi.org/10.1210/endo.136.9.7649105

Han, J., Jeong, W., Gu, M. J., Yoo, I., Yun, C. H., Kim, J., & Ka, H. (2018). Cysteine-X-cysteine motif chemokine ligand 12 and its receptor CXCR4: Expression, regulation, and possible function at the maternal-conceptus interface during early pregnancy in pigs. *Biology of Reproduction*, 99(6), 1137–1148. https://doi.org/10.1093/biolre/ioy147

Hanna, V. S., & Hafez, E. A. A. (2018). Synopsis of arachidonic acid metabolism: A review. *Journal of Advanced Research*, 11, 23–32. https://doi.org/10.1016/j.jare.2018.03.005

Hettinger, A. M., Allen, M. R., Zhang, B. R., Goad, D. W., Malayer, J. R., & Geisert, R. D. (2001). Presence of the acute phase protein, bikunin, in the endometrium of gilts during estrous cycle and early pregnancy. *Biology of Reproduction*, 65(2), 507–513. https://doi.org/10.1095/biolreprod65.2.507

Hong, C., Duit, S., Jalonen, P., Out, R., Scheer, L., Sorrentino, V., Boyadjian, R., Rodenburg, K. W., Foley, E., Korhonen, L., Lindholm, D., Nimpf, J., Van Berkel, T. J. C., Tontonoz, P., & Zelcer, N. (2010). The E3 ubiquitin ligase IDOL induces the degradation of the low density lipoprotein receptor family members VLDLR and ApoER2. *Journal of Biological Chemistry*, 285(26), 19720–19726. https://doi.org/10.1074/jbc.M110.123729

Horibata, Y., & Hirabayashi, Y. (2007). Identification and characterization of human ethanolaminephosphotransferase1. *Journal of Lipid Research*, 48(3), 503–508. https://doi.org/10.1194/jlr.C600019-JLR200

Jeong, W., Song, G., Bazer, F. W., & Kim, J. (2014). Insulin-like growth factor I induces proliferation and migration of porcine trophectoderm cells through multiple cell signaling pathways, including protooncogenic protein kinase 1 and mitogen-activated protein kinase. *Molecular and Cellular Endocrinology*, 384(1-2), 175–184. https://doi.org/10.1016/j.mce.2014.01.023

Ka, H., Jaeger, L. A., Johnson, G. A., Spencer, T. E., & Bazer, F. W. (2001). Keratinocyte growth factor is up-regulated by estrogen in the porcine uterine endometrium and functions in trophectoderm cell proliferation and differentiation. *Endocrinology*, 142(6), 2303–2310. https://doi.org/10.1210/endo.142.6.8194

Kayser, J. -P. R., Kim, J. G., Cerny, R. L., & Vallet, J. L. (2006). Global characterization of porcine intrauterine proteins during early pregnancy. *Reproduction*, 131(2), 379–388. https://doi.org/10.1530/rep.1.00882

Kim, D., Langmead, B., & Salzberg, S. L. (2015). HISAT: A fast spliced aligner with low memory requirements. *Nature Methods*, 12(4), 357–360. https://doi.org/10.1038/nmeth.3317

Kim, T. J., Mitsutake, S., & Igarashi, Y. (2006). The interaction between the pleckstrin homology domain of ceramide kinase and phosphatidylinositol 4,5-bisphosphate regulates the plasma membrane targeting and ceramide 1-phosphate levels. *Biochemical and Biophysical Research Communications*, 342(2), 611–617. https://doi.org/10.1016/j.bbrc.2006.01.170

Kumari, M., Schoiswohl, G., Chitraju, C., Paar, M., Cornaciu, I., Rangrez, A. Y., Wongsiriroj, N., Nagy, H. M., Ivanova, P. T., Scott, S. A., Knittelfelder, O., Rechberger, G. N., Birner-Gruenberger, R., Eder, S., Brown, H. A., Haemmerle, G., Oberer, M., Lass, A., Kershaw, E. E., … Zechner, R. (2012). Adiponutrin functions as a nutritionally regulated lysophosphatidic acid acyltransferase. *Cell Metabolism*, 15(5), 691–702. https://doi.org/10.1016/j.cmet.2012.04.008

Lahiri, S., Lee, H., Mesicek, J., Fuks, Z., Haimovitz-Friedman, A., Kolesnick, R. N., & Futerman, A. H. (2007). Kinetic characterization of mammalian ceramide synthases: Determination of K(m) values towards sphinganine. *FEBS Letters*, 581(27), 5289–5294. https://doi.org/10.1016/j.febslet.2007.10.018

Laughlin, T. D., Miles, J. R., Wright-Johnson, E. C., Rempel, L. A., Lents, C. A., & Pannier, A. K. (2017). Development of pre-implantation porcine blastocysts cultured within alginate hydrogel systems either supplemented with secreted phosphoprotein 1 or conjugated with Arg-Gly-Asp Peptide. *Reproduction, Fertility, and Development*, 29(12), 2345–2356. https://doi.org/10.1071/RD16366

Lee, S. H., Zhao, S. -H., Recknor, J. C., Nettleton, D., Orley, S., Kang, S. -K., Lee, B. -C., Hwang, W. -S., & Tuggle, C. K. (2005). Transcriptional

profiling using a novel cDNA array identifies differential gene expression during porcine embryo elongation. *Molecular Reproduction and Development*, 71(2), 129–139. https://doi.org/10.1002/mrd.20291

Love, M. I., Huber, W., & Anders, S. (2014). Moderated estimation of fold change and dispersion for RNA-seq data with DESeq. 2. *Genome Biology*, 15(12), 550. https://doi.org/10.1186/s13059-014-0550-8

Massuto, D. A., Hooper, R. N., Kneese, E. C., Johnson, G. A., Ing, N. H., Weeks, B. R., & Jaeger, L. A. (2010). Intrauterine infusion of latency-associated peptide (LAP) during early porcine pregnancy affects conceptus elongation and placental size. *Biology of Reproduction*, 82(3), 534–542. https://doi.org/10.1095/biolreprod.109.081893

McLeod, R. S., & Yao, Z. (2016). Assembly and secretion of triglyceride-rich lipoproteins. In N. D. Ridgway, & R. S. McLeod (Eds.), *Biochemistry of Lipids, Lipoproteins and Membranes* (6th ed., pp. 459–488). Elsevier. https://doi.org/10.1016/B978-0-444-63438-2.00016-X

Miles, J. R., Freking, B. A., Blomberg, L. A., Vallet, J. L., & Zuelke, K. A. (2008). Conceptus development during blastocyst elongation in lines of pigs selected for increased uterine capacity or ovulation rate. *Journal of Animal Science*, 86(9), 2126–2134. https://doi.org/10.2527/jas.2008-1066

Nagaoka, A., Yoshida, H., Nakamura, S., Morikawa, T., Kawabata, K., Kobayashi, M., Sakai, S., Takahashi, Y., Okada, Y., & Inoue, S. (2015). Regulation of hyaluronan (HA) metabolism mediated by HYBID (hyaluronan-binding protein involved in HA depolymerization, KIAA1199) and HA synthases in growth factor-stimulated fibroblasts. *Journal of Biological Chemistry*, 290(52), 30910–30923. https://doi.org/10.1074/jbc.M115.673566

Payton, J. E., Perrin, R. J., Woods, W. S., & George, J. M. (2004). Structural determinants of PLD2 inhibition by α-synuclein. *Journal of Molecular Biology*, 337(4), 1001–1009. https://doi.org/10.1016/j.jmb.2004.02.014

Pertea, M., Pertea, G. M., Antonescu, C. M., Chang, T. C., Mendell, J. T., & Salzberg, S. L. (2015). StringTie enables improved reconstruction of a transcriptome from RNA-seq reads. *Nature Biotechnology*, 33(3), 290–295. https://doi.org/10.1038/nbt.3122

Pope, W. F., & First, N. L. (1985). Factors affecting the survival of pig embryos. *Theriogenology*, 23(1), 91–105. https://doi.org/10.1016/0093-691X(85)90075-5

Pope, W. F. (1994). Embryonic mortality in swine. In M. T. Zavy, & R. D. Geisert (Eds.), *Embryonic mortality in domestic species* (pp. 53–77). CRC Press.

Powell, J. K., Glasser, S. R., Woldesenbet, S., Burghardt, R. C., & Newton, G. R. (2000). Expression of carbohydrate antigens in the goat uterus during early pregnancy and on steroid-treated polarized uterine epithelial cells in vitro. *Biology of Reproduction*, 62(2), 277–284. https://doi.org/10.1095/biolreprod62.2.277

Powell, W. S., & Rokach, J. (2015). Biosynthesis, biological effects, and receptors of hydroxyeicosatetraenoic acids (HETEs) and oxoeicosatetraenoic acids (oxo-ETEs) derived from arachidonic acid. *Biochimica et Biophysica Acta*, 1851(4), 340–355. https://doi.org/10.1016/j.bbalip.2014.10.008

Prasad, S. S., Garg, A., & Agarwal, A. K. (2011). Enzymatic activities of the human AGPAT isoform 3 and isoform 5: Localization of AGPAT5 to mitochondria. *Journal of Lipid Research*, 52(3), 451–462. https://doi.org/10.1194/jlr.M007575

Raheem, K. A. (2018). Cytokines, growth factors and macromolecules as mediators of implantation in mammalian species. *International Journal of Veterinary Science and Medicine*, 6, S6–S14. https://doi.org/10.1016/j.ijvsm.2017.12.001

Ribeiro, E. S., Santos, J. E. P., & Thatcher, W. W. (2016). Role of lipids on elongation of the preimplantation conceptus in ruminants. *Reproduction*, 152(4), R115–R126. https://doi.org/10.1530/REP-16-0104

Ross, J. W., Ashworth, M. D., Hurst, A. G., Malayer, J. R., & Geisert, R. D. (2003). Analysis and characterization of differential gene expression during rapid trophoblastic elongation in the pig using suppression subtractive hybridization. *Reproductive Biology and Endocrinology*, 1(23), 1–12. https://doi.org/10.1186/1477-7827-1-23

Ross, J. W., Ashworth, M. D., Stein, D. R., Couture, O. P., Tuggle, C. K., & Geisert, R. D. (2009). Identification of differential gene expression during porcine conceptus rapid trophoblastic elongation and attachment to uterine luminal epithelium. *Physiological Genomics*, 36(3), 140–148. https://doi.org/10.1152/physiolgenomics.00022.2008

Ross, J. W., Malayer, J. R., Ritchey, J. W., & Geisert, R. D. (2003). Characterization of the interleukin-1β system during porcine trophoblastic elongation and early placental attachment. *Biology of Reproduction*, 69(4), 1251–1259. https://doi.org/10.1095/biolreprod.103.015842

Schaloske, R. H., & Dennis, E. A. (2006). The phospholipase A2 superfamily and its group numbering system. *Biochimica et Biophysica Acta*, 1761(11), 1246–1259. https://doi.org/10.1016/j.bbalip.2006.07.011

Shulga, Y. V., Topham, M. K., & Epand, R. M. (2011). Regulation and functions of diacylglycerol kinases. *Chemical Reviews*, 111(10), 6186–6208. https://doi.org/10.1021/cr1004106

Simmons, R. M., Satterfield, M. C., Welsh, T. H., Bazer, F. W., & Spencer, T. E. (2010). HSD11B1, HSD11B2, PTGS2, and NR3C1 expression in the peri-implantation ovine uterus: Effects of pregnancy, progesterone, and interferon tau. *Biology of Reproduction*, 82(1), 35–43. https://doi.org/10.1095/biolreprod.109.079608

Stojkovic, M., Krebs, O., Kölle, S., Prelle, K., Assmann, V., Zakhartchenko, V., Sinowatz, F., & Wolf, E. (2003). Developmental regulation of hyaluronan-binding protein (RHAMM/IHABP) expression in early bovine embryos. *Biology of Reproduction*, 68(1), 60–66. https://doi.org/10.1095/biolreprod.102.007716

Strauss, J. F., & FitzGerald, G. A. (2019). Steroid hormones and other lipid molecules involved in human reproduction. In J. F. Strauss, & R. L. Barbieri (Eds.), *Yen & Jaffe's reproductive endocrinology: Physiology, pathophysiology, and clinical management* (8th ed., pp. 75–114). Elsevier. https://doi.org/10.1016/B978-0-323-47912-7.00004-4

Tafesse, F. G., Huitema, K., Hermansson, M., van der Poel, S., van den Dikkenberg, J., Uphoff, A., Somerharju, P., & Holthuis, J. C. M. (2007). Both sphingomyelin synthases SMS1 and SMS2 are required for sphingomyelin homeostasis and growth in human HeLa cells. *Journal of Biological Chemistry*, 282(24), 17537–17547. https://doi.org/10.1074/jbc.M702423200

Takahashi, T., & Suzuki, T. (2012). Role of sulfatide in normal and pathological cells and tissues. *Journal of Lipid Research*, 53(8), 1437–1450. https://doi.org/10.1194/jlr.R026682

Tsuboi, K., Okamoto, Y., Rahman, I. A. S., Uyama, T., Inoue, T., Tokumura, A., & Ueda, N. (2015). Glycerophosphodiesterase GDE4 as a novel lysophospholipase D: A possible involvement in bioactive N-acylethanolamine biosynthesis. *Biochimica et Biophysica Acta*, 1851(5), 537–548. https://doi.org/10.1016/j.bbalip.2015.01.002

Vallet, J. L., Miles, J. R., & Freking, B. A. (2009). Development of the pig placenta. *Society of Reproduction and Fertility supplement*, 66, 265–279.

Waclawik, A., Kaczmarek, M. M., Blitek, A., Kaczynski, P., & Ziecik, A. J. (2017). Embryo-maternal dialogue during pregnancy establishment and implantation in the pig. *Molecular Reproduction and Development*, 84(9), 842–855. https://doi.org/10.1002/mrd.22835

Walsh, S. C., Miles, J. R., Yao, L., Broeckling, C. D., Rempel, L. A., Wright-Johnson, E. C., & Pannier, A. K. (2020). Metabolic compounds within the porcine uterine environment are unique to the type of conceptus present during the early stages of blastocyst elongation. *Molecular Reproduction and Development*, 87(1), 174–190. https://doi.org/10.1002/mrd.23306

Xu, R., Jin, J., Hu, W., Sun, W., Bielawski, J., Szulc, Z., Taha, T., Obeid, L. M., & Mao, C. (2006). Golgi alkaline ceramidase regulates cell proliferation and survival by controlling levels of sphingosine and S1P. *FASEB Journal*, *20*(11), 1813–1825. https://doi.org/10.1096/fj.05-5689com

Yelich, J. V., Pomp, D., & Geisert, R. D. (1997a). Detection of transcripts for retinoic acid receptors, retinol-binding protein, and transforming growth factors during rapid trophoblastic elongation in the porcine conceptus. *Biology of Reproduction*, *57*(2), 286–294. https://doi.org/10.1095/biolreprod57.2.286

Yelich, J. V., Pomp, D., & Geisert, R. D. (1997b). Ontogeny of elongation and gene expression in the early developing porcine conceptus. *Biology of Reproduction*, *57*(5), 1256–1265. https://doi.org/10.1095/biolreprod57.5.1256

Yen, C. L. E., Stone, S. J., Cases, S., Zhou, P., & Farese, R. V. (2002). Identification of a gene encoding MGAT1, a monoacylglycerol acyltransferase. *Proceedings of the National Academy of Sciences of the United States of America*, *99*(13), 8512–8517. https://doi.org/10.1073/pnas.132274899

Yen, M. C., Chou, S. K., Kan, J. Y., Kuo, P. L., Hou, M. F., & Hsu, Y. L. (2019). New insight on solute carrier family 27 member 6 (SLC27A6) in tumoral and non-tumoral breast cells. *International Journal of Medical Sciences*, *16*(3), 366–375. https://doi.org/10.7150/ijms.29946

Zang, X., Gu, T., Hu, Q., Xu, Z., Xie, Y., Zhou, C., Zheng, E., Huang, S., Xu, Z., Meng, F., Cai, G., Wu, Z., & Hong, L. (2021). Global transcriptomic analyses reveal genes involved in conceptus development during the implantation stages in pigs. *Frontiers in Genetics*, *12*, 584995. https://doi.org/10.3389/fgene.2021.584995

Zeng, S., Bick, J., Kradolfer, D., Knubben, J., Flöter, V. L., Bauersachs, S., & Ulbrich, S. E. (2019). Differential transcriptome dynamics during the onset of conceptus elongation and between female and male porcine embryos. *BMC Genomics*, *20*(1), 679. https://doi.org/10.1186/s12864-019-6044-z

Zheng, Z., Li, Y., Jin, G., Huang, T., Zou, M., & Duan, S. (2020). The biological role of arachidonic acid 12-lipoxygenase (ALOX12) in various human diseases. *Biomedicine and Pharmacotherapy*, *129*, 110354. https://doi.org/10.1016/j.biopha.2020.110354

Ziecik, A. J., Waclawik, A., Kaczmarek, M. M., Blitek, A., Jalali, B. M., & Andronowska, A. (2011). Mechanisms for the establishment of pregnancy in the pig. *Reproduction in Domestic Animals*, *46*(s3), 31–41. https://doi.org/10.1111/j.1439-0531.2011.01843.x

SUPPORTING INFORMATION

Additional supporting information may be found in the online version of the article at the publisher's website.